Cloning and characterization of genes involved in Fe-homeostasis in graminaceous plants

イネ科植物の鉄-ホメオスタシスに関わる遺伝子の単離と解析

Bashir Khurram

Table of Contents

Acknowledgement

First of all I am thankful to Japanese Government and MEXT for providing me a chance to conduct my PhD studies at The University of Tokyo and financially supporting me during the course of Study. I have enjoyed my stay in Japan and The University of Tokyo. The environment of our lab is excellent for research work and all the credit goes to Prof. Dr. Naoko Nishizawa. She is very kind cooperative, and helping. I always feel lucky for working under her supervision. I am also thankful to Prof. Emirates Dr. Satoshi Mori for his guidance throughout the course of this study. I also would like to thank Dr. Hiromi Nakanishi and Dr. Michiko Takahashi for their time and useful suggestions to improve my research. Practically, Dr. Nagasaka spared a lot of time to teach me molecular techniques and helping me throughout the experiments. He has not only guided me in lab but also helped me to solve my daily life problems. His extraordinary favor is a major inspiration for this contribution. I am also thankful to Dr. Haruhiko Inoue, Dr. Takanori Kobayashi and Dr. Yasuhiro Ishimaru for their suggestions, guidance and help during this research. I would like to take this chance to pay thanks to my colleagues especially, Mr. Motofumi Suzuki, Mrs. Reiko N. Itai, Ms Yuko Ogo, Dr. Tomoko Nozoye and others for helping time to time. This acknowledgement will be incomplete if I would not mention the moral support provided by my family especially my parents and my wife, Sultana Khurram. Finally I am thankful again to my Supervisor, Prof. Dr. Naoko Nishizawa for her excellent guidance through the course of study and encouraging me to finish my research in time.

Khurram Bashir

List of Figures

List of Tables

List of Abbreviations

AKR:	Aldo-keto reductase super family
DMA:	Deoxymugineic acid
DMAS:	DMA synthase
Fe:	Iron
GR:	Glutathione reductase
GSH:	Glutathione
GT:	Glutathione transporter
GTL:	Glutathione transporter like
MAs:	Mugineic acid family phytosiderophores
NA:	Nicotianamine
NAAT:	NA amino transferase
OPT:	Oligopeptide transporter
YSL:	Yellow stripe like

Summary

Summary

Iron (Fe) is an essential element required for various cellular events in plants, including respiration, chlorophyll biosynthesis, and photosynthetic electron transport. Fe is also a component of the Fe-S cluster, which is present in numerous enzymes. Thus the acquisition of Fe from soil and its homeostasis is essential for normal plant growth. To understand the mechanisms of Fe acquisition and homeostasis, different genes involved in Fe-acquisition/homeostasis or Fe-deficiency induced stress tolerance were cloned from graminaceous plants. These include deoxymugineic acid synthase (DMAS) from rice (*OsDMAS1*), barley (*HvDMAS1*), wheat (*TaDMAS1*) and maize (*ZmDMAS1*) plants, glutathione reductase (GR) from barley (*HvGR1* and *HvGR2*) and glutathione transporter like gene (*OsGTL1*) from rice. The expression patterns of these genes and their possible roles in Fe-acquisition as well as homeostasis were investigated.

1). **Cloning and characterization of DMAS genes from graminaceous plants**

Graminaceous plants have evolved a unique mechanism to acquire Fe and secrete a family of small molecules, called mugineic acid family phytosiderophores (MAs) in response to Fe-deficiency. MAs are synthesized from L-methionine. Three molecules of S-adenosyl methionine are combined together to form one molecule of nicotianamine (NA). The amino group of NA is transferred by NA-amino transferase to form 3"-keto intermediate, which is subsequently reduced to

deoxymugineic acid (DMA) by DMA synthase (DMAS). DMA is the first member of MAs and MAs share the same pathway from L-methionine to DMA and the subsequent steps may differ depending upon the plant species and even cultivars. Previously all the genes with the exception of DMAS, involved in MAs biosynthetic pathway have been cloned from rice and barley. *DMAS* was first isolated from rice (*OsDMAS1*) as a member of aldo-keto reductase super family (AKR) upregulated under Fe-deficiency and then its orthologs from barley (*HvDMAS1*), wheat (*TaDMAS1*), and maize (*ZmDMAS1*) were also cloned. Their nucleotide sequences indicate that *OsDMAS1* encodes a predicted polypeptide of 318 amino acids, whereas the other three orthologs all encode predicted polypeptides of 314 amino acids and are highly homologous (82-97.5%) to each other. The *DMAS* genes belong to AKR and have homology to *Papaver somniferum* codeinone reductases (AKR4B2-3), and *Medicago sativa* (AKR4A2) and *Glycine max* (AKR4A1) chalcone polyketide reductases. Although strictly speaking it does not fall in to existing subfamilies of AKR4, however, after introduction of conservative substitutions, the identity with existing members of AKR4B reached up to 65% and ZmDMAS1, OsDMAS1, HvDMAS1 and TaDMAS1 were assigned the numbers from AKR4B5 to AKR4B8 respectively. DMAS proteins were expressed in *E. coli.* as maltose binding fusion proteins and all the recombinant proteins showed DMA synthesis activity *in vitro*. Their enzymatic activities were highest at pH 8 to 9, consistent with the hypothesis that DMA is synthesized in subcellular vesicles. Northern blot analysis revealed that the expression of each of the above *DMAS* genes is

upregulated under Fe-deficient conditions in root tissue, and that of *OsDMAS1* and *TaDMAS1* are upregulated in shoot tissue. Western blot analysis confirmed that expression of DMAS is upregulated under Fe-deficiency. Moreover, it seems that low expression of DMAS is a rate limiting factor responsible for the low production of MAs in rice. *OsDMAS1* promoter-*GUS* analysis in Fe-sufficient roots showed that its expression is restricted to cells participating in long-distance transport, and that it is highly upregulated in entire root under Fe-deficient conditions. In shoot tissue, *OsDMAS1* promoter drove expression in vascular bundles specifically under Fe-deficient conditions. With the cloning of graminaceous DMAS, all the genes of MA biosynthetic pathway have been cloned from barley and rice. The cloning of DMAS is an important step in understanding the Fe acquisition and will help to develop transgenic rice highly tolerant to Fe-deficiency in alkaline soils.

2). Cloning and characterization of glutathione reductase from barely

Glutathione reductase (GR) plays an important role in the response to biotic and abiotic stresses in plants like salt stress, high temperature, low temperature and pathogen attack. Although GR is also involved in response to Fe-toxicity, little is known about expression patterns of GR under Fe-deficient conditions. The expression patterns and enzyme activities of GR in graminaceous plants under Fe-sufficient and Fe-deficient conditions were examined by isolating cDNA clones for chloroplastic GR (*HvGR1*) and cytosolic GR (*HvGR2*) from barley. It was found that the sequences of *GR1* and *GR2* were highly conserved in graminaceous plants.

Based on their nucleotide sequences, *HvGR1* and *HvGR2* were predicted to encode polypeptides of 550 and 497 amino acids, respectively. Both proteins showed *in vitro* GR activity, and the specific activity for HvGR1 was threefold that of HvGR2. Northern blot analyses were performed to examine the expression patterns of GR1 and GR2 in rice (*Oryza sativa*), wheat (*Triticum aestivum*), barley (*Hordeum vulgare*), and maize (*Zea mays*). *HvGR1*, *HvGR2*, and *TaGR2* were upregulated in response to Fe-deficiency. Moreover, *HvGR1* and *TaGR1* were mainly expressed in shoot tissues, whereas *HvGR2* and *TaGR2* were primarily observed in root tissues. It was observed that the expression of *HvGR2* follows a diurnal rhythm in Fe-sufficient and Fe-deficient plants. The GR activity increased in roots of barley, wheat, and maize and shoot tissues of rice, barley, and maize in response to Fe-deficiency. Furthermore, it appeared that GR was not posttranscriptionally regulated, at least in rice, wheat, and barley. These results suggest that GR may play a role in the Fe-deficiency induced stress response in graminaceous plants.

3). Cloning and characterization of Os*GTL1*

Glutathione (GSH) is involved in many aspects of plant growth and development including redox control, storage and transport of reduced sulfur, and response to biotic and abiotic stresses. The transport and compartmentalization of GSH is essential to perform all these functions. A GSH transporter (GT) like genes was cloned from rice (*OsGTL1*) to understand its role in mitigating Fe-deficiency

stress. *OsGTL1* is a putative member of oligopeptide transporters (OPT) family, and was identified through microarray analysis as its expression was highly upregulated in response to Fe-deficiency in root and shoot tissue. *OsGTL1* was predicted to encode a polypeptide of 757 amino acids containing 12 putative transmembrane domains. It contains the NPG domain (NPGPFxxKEH) and KP domain (KLGHYMKIPPR) earlier identified in AtOPTs. Seven homologs of *OsGTL1* were identified in rice including previously characterized *OsGT1*. *OsGTL1* showed high homology i.e. 82% homology to *BjGT1* and 80% homology to *AtOPT3*. Northern blot analysis confirmed that the expression of *OsGTL1* is induced in response to Fe deficiency. OsGTL1-green fluorescent protein (GFP) was localized to the plasma membrane of onion epidermal cell. Electrophysiological measurements using *Xenopus leavis* oocytes showed that OsGTL1 is a functional GSH transporter. GUS expression driven by *OsGTL1* promoter was not observed in Fe-sufficient roots. In contrast, in Fe-deficient roots, high level of *OsGTL1* promoter derived GUS expression was observed near root tips and the expression diluted as the distance from root tip increased. In shoot tissue, *OsGTL1* promoter's expression was observed in whole leaf under Fe-deficient and specifically in vascular bundle under Fe-sufficient conditions. These results suggested that *OsGTL1* is a novel glutathione transporter up-regulated under Fe-deficient conditions and may play a critical role in Fe-deficiency induced stress in rice.

CHAPTER

1

Introduction

1). Introduction

Rice (*Oryza sativa* L.) is one of the most important food crops feeding more than 2 billion people in Asia (FAO, 1995). Rice provides 27% of dietary energy supply and 20% of dietary protein intake over all (Anonymous, 2003). Rice is life for major populations of the world and is deeply embedded in the cultural heritage of societies. The world population was 6 billion in the year 2000, will increase to 10 billion by 2025, expecting in the increase of rice consumers by two fold by the year 2020 (Khush and Toenniessen, 1991). Improving the productivity of rice systems would contribute to hunger eradication, poverty alleviation, national food security and economic development. Rice productivity is affected by several abiotic and biotic factors including mineral deficiency. Thus, understanding the mechanisms of mineral nutrition can help to increase the crop production. At the same time, this knowledge may be useful to increase the mineral contents in edible parts of crop plants and ultimately mitigating the mineral deficiency in humans. Among mineral deficiencies Fe-deficiency is a major problem affecting a larger proportion of the world. According to world health organization (WHO) about 60% to 80% of the world population suffers in Fe-deficiency in some manner (World Health Organization, 2002). Thus, it is extremely important to understand the mechanisms of Fe-uptake from soils and its homeostasis in plants. This knowledge could help to breed crops, tolerant to Fe-deficiency stress and accumulating more Fe in edible parts to overcome Fe-deficiency in humans.

Iron (Fe) is an important mineral nutrient. Although required in small amount, Fe is an essential element required for various cellular events in plants including respiration, chlorophyll biosynthesis, and photosynthetic electron transport. Fe is also a component of the Fe-S cluster, which is present in numerous enzymes. Thus the acquisition of Fe from soil and its homeostasis is essential for normal plant growth. Fe-deficiency causes a metabolic imbalance deleterious to plant development (Briat et al., 1995). Being the fourth most abundant mineral element, Fe comprises about 5% of the earth's crust. However, its bioavailability is a problem in many regions especially in alkaline soils (pH>7), common in semiarid and arid climates. Calcareous soils cover more than 30% of the world surface (Chen and Barak, 1982) and soils are common in Pakistan and India. Their content of $CaCO_3$ in the upper horizon varies from a few percent to 95%. In calcareous soils, the high pH dislocates the chemical balance towards the formation of Fe insoluble complexes, leaving the cation sparsely available for plant uptake (Guerinot and Yi, 1994; Briat et al., 1995). However, in anaerobic conditions and acid pH, as found in waterlogged soils, the ferrous form is stabilized and readily taken up by plants. When in excess, Fe induces the production of hydroxyl radicals, which cause damage to cellular structures (Guerinot and Yi, 1994; Briat et al., 1995). So the Fe uptake and homeostasis should be under strict regulation for normal plant growth and development. Plants have developed sophisticated mechanisms for Fe uptake and homeostasis which can be divided in two broad categories (Marschner and Römheld, 1994).

All plants, except graminaceous monocots (Strategy I), release protons to acidify the rhizosphere and secrete reductants/chelators such as organic acids and phenolics (Römheld and Marschner, 1983; Römheld et al., 1984). The ferric ion is then chelated by the released compounds, as well as by soil bacteriosiderophores (Römheld and Marschner, 1983; Bar-Ness et al., 1992). Subsequently, chelated Fe^{+3} is reduced by ferric chelate reductase at the plasma membrane of root epidermal cells (Moog and Bruggermann, 1994) and Fe^{+2} is then absorbed by roots.. On the other hand graminaceous monocots (strategy II plants) release mugineic acid family phytosiderophores (MAs), to solubilize soil Fe (Takagi, 1976; Takagi et al., 1984) and the resultant Fe(III)-MAs complex is readily absorbed by the plant through a specific transporter (Curie et al., 2001).

MAs are synthesized from L-Met (Mori and Nishizawa, 1987). Nicotianamine synthase (NAS) catalyzes the trimerization of S-adenosyl Met (SAM) molecules to form nicotianamine (NA) (Higuchi et al., 1994; Higuchi et al., 1999), which is then converted into a 3"-keto intermediate by the transfer of an amino group by nicotianamine aminotransferase (NAAT) (Kanazawa et al., 1994). The subsequent reduction of the 3"-carbon of the keto intermediate produces 2'-deoxymugineic acid (DMA). DMA is the first MA synthesized in the pathway. The biosynthetic pathway of all MAs is the same from L-Met to DMA, but the subsequent steps differ depending on the plant species or even the cultivar (Ma et al., 1999). To date nine kinds of MAs have been identified (Nomoto et al., 1987; Ma et al., 1999; Ueno et al., 2004) and their biosynthetic pathways have been investigated both *in vivo* (Mori

and Nishizawa, 1987, 1989; Kawai et al., 1988; Mori et al., 1990; Ma and Nomoto, 1993; Ma et al., 1999) and *in vitro* (Shojima et al., 1989; 1990). The production and secretion of MAs markedly increases in response to Fe deficiency, and tolerance to Fe deficiency in graminaceous plants is strongly correlated with MAs secreted. Barley secretes mugineic acid (MA), 3-epihydroxy-2'-deoxymugineic acid (EpiHDMA), and 3-epihydroxy mugineic acid (EpiHMA), in addition to DMA. Rye secretes DMA, MA, and 3-hydroxy mugineic acid (HMA), while oat secretes DMA and avenic acid. Rice, wheat, maize, and sorghum usually secrete only DMA although some kinds of ancestral wheat also secrete unknown MAs.

Transformation of crop plants to increase their capacity to enhance the Fe content may result in yield improvement (Takahashi et al., 2001; Guerinot, 2001). For example for Fe-deficiency tolerance, introduction of the barley genes of MAs biosynthetic pathway into rice could result in increased tolerance to Fe-deficiency stress (Takahashi et al., 2001; Takahashi, 2003). The increase in Fe content in plant staple foods can minimize human nutritional problems (Murrey-Kolb et al., 2002). In this regard, a better understanding of Fe homeostasis, involving knowledge of the basic physiological processes of Fe absorption, distribution and storage in plants, can serve as starting point for the manipulation of crops through biotechnology (Grusak, 2002; Grotz and Guerinot, 2002). Besides Fe acquisition from soil, it is also important to investigate the response of crop plants to Fe-deficiency induced stress. This may include identification of new genes

upregulated in response to Fe-deficiency and characterization of previously identified genes to understand their role in mitigating Fe-deficiency stress.

Present studies were designed to isolate and characterize the genes participating directly or indirectly in response to Fe-deficiency stress. Two different strategies were employed to clone the genes participating in Fe-deficiency response in graminaceous crops. At one hand a full length cDNA library prepared from Fe-deficient barely roots was screened with a previously identified cDNA clone (AB063249) and full length cDNA clone for cytosolic glutathione reductase (GR) was isolated. Afterwards the chloroplastic GR was also isolated and enzyme activity and expression patterns were characterized in graminaceous plants. The results indicated that GR may have a role in response to Fe-deficiency stress in graminaceous plants. On the other hand microarray analysis were used to identify the genes upregulated under Fe-deficiency stress and a gene for DMA synthase (DMAS) was identified in rice and its orthologs were cloned form graminaceous plants i.e. barely, wheat and maize. The expression and enzyme activities of these clones were studies. Finally, *Oryza sativa* glutathione transporter like-1 gene (*OsGTL1*) in rice was identified and characterized. Although graminaceous *DMAS*s, *HvGR* and *OsGTL1* have no direct relation, they are important for Fe-deficiency response of plants. Interestingly, the genes for chloroplastic GR, *OsGTL1* and *DMAS* reside on rice chromosome 3. The characterization of these genes will help to understand the Fe acquisition and to develop strategies to mitigate Fe-deficiency in plants and humans.

CHAPTER

2

Cloning and Characterization of *DMAS* Genes from Graminaceous Plants

2.1) Introduction

Iron (Fe) is an essential element that is required for various cellular events in plants, including respiration, chlorophyll biosynthesis, and photosynthetic electron transport. Fe is also a component of the Fe-S cluster, which is present in numerous enzymes. Although soil contains abundant Fe, it is mainly present as oxidized Fe(III) compounds, which are poorly soluble in neutral to alkaline soils. Therefore, plants have developed sophisticated and tightly regulated mechanisms for acquiring Fe from the soil, which can be grouped into two strategies as discussed in **section-1**. Graminaceous plants solubilize soil Fe by secreting MAs, from their roots (Takagi, 1976; Takagi et al., 1984). The resulting Fe(III)-MAs complexes are then reabsorbed into the roots through a specific transporter. The production and secretion of MAs markedly increases in response to Fe deficiency, and tolerance to Fe deficiency in graminaceous plants is strongly correlated with the quantity and quality of the MAs secreted. For example, rice, wheat, and maize secrete only 2'-deoxymugineic acid (DMA) in relatively low amounts and are thus susceptible to low Fe availability. In contrast, barley secretes large amounts of many types of MAs, including mugineic acid (MA), 3-hydroxymugineic acid (HMA), and 3-epi-hydroxymugineic acid (epi-HMA), and is therefore more tolerant to low Fe availability (Römheld and Marschner 1990; Singh et al., 1993).

The biosynthetic pathway for MAs has already been characterized (**Fig-2.1**). With the exception of DMA synthase (DMAS), almost all of the genes involved in the biosynthetic pathway for MAs have been isolated and characterized (Higuchi et

al., 1999; Takahashi et al., 1999; Okumura et al., 1994; Nakanishi et al., 1993; Nakanishi et al., 2000; Kobayashi et al., 2001). A gene that encodes an Fe(III)-MA transporter, Yellow Stripe1 (*YS1*), has been isolated from maize (Curie et al., 2001). The *YS1* mRNA level increases in both roots and shoots, under Fe-deficient conditions. *YS1*-like genes also exist in rice (Koike et al., 2004). The expression of the genes involved in the biosynthetic pathway of MAs is dramatically enhanced by Fe deficiency in barley (Higuchi et al., 1999; Takahashi et al., 1999; enhanced by Fe deficiency in barley (Higuchi et al., 1999;Takahasi et al., 1999; Okumura et al., 1994; Nakanishi et al., 1993; Nakanishi et al., 2000; Neigishi et al., 2002) rice (Higuchi et al., 2001; Inoue et al., 2003; Kobayashi et al., 2005) and maize (Mizuno et al., 2003), resulting in increased secretion of MAs. All of the barley Fe-deficiency-inducible genes that have been isolated are expressed almost exclusively in roots, suggesting that the root-specific expression of these genes is important for the strong tolerance of barley to Fe deficiency, whereas many Fe-deficiency-inducible genes in rice are expressed in both roots and shoots. In spite of all these advances, the isolation of the gene responsible for the conversion of the 3"-keto intermediate to DMA has not been reported previously. One objective of the present studies was to clone DMAS genes from graminaceous crops, especially form barley and to characterize its expression patterns under Fe-deficient conditions. Finally, the cloning of *DMAS* genes from rice (*OsDMAS1*), barley (*HvDMAS1*), wheat (*TaDMAS1*), and maize (*ZmDMAS1*) is reported here. The sequences of proteins in this subfamily are highly conserved in graminaceous

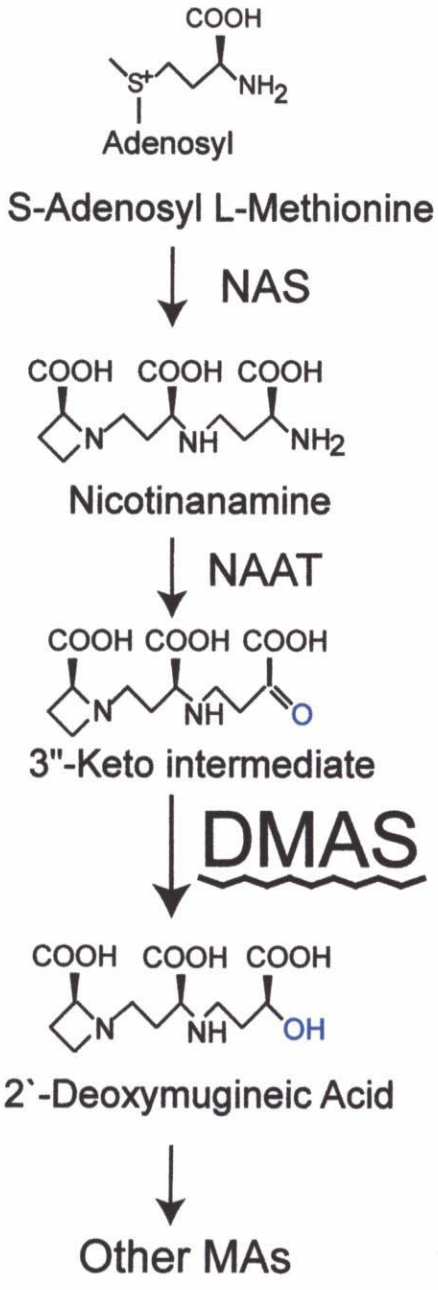

Fig-2.1: Biosynthetic Pathway of Mugineic Acid Family Phytosiderophores

Three molecules of S-adenosyl methionine are combined by NA synthase (NAS) to form nicotianamine (NA). The amino group of NA is transferred by NA aminotransferase (NAAT), and the resultant 3"-keto intermediate is reduced to 2'-deoxymugineic acid (DMA) by DMA synthase (DMAS). The subsequent steps differ with the plant species and cultivar.

plants. It seems that low expression of DMAS is rice is major factor for its low tolerance to Fe-deficiency in alkaline soils. The isolation of the *DMAS* gene from barley, one of the graminaceous plants most tolerant to Fe deficiency, is an important step in the production of transgenic rice lines highly tolerant to Fe deficiency.

2.2). Experimental procedures

2.2.1). Isolation of *DMAS* genes

Two different strategies were used to clone DMAS (**Fig-2.2**). First, degenerate primers were designed for the conserved regions of oxidoreductase to amplify cDNA clones induced under Fe-deficient conditions. Secondly, analysis of a rice 22-k custom oligo DNA microarray containing the sequence data from the rice full-length cDNA project (Ogo et al., 2006) was used to identify *OsDMAS1* (AK073738; putative NADPH-dependent oxidoreductase) as a putative member of the aldo-keto reductase superfamily (AKR), which is induced under Fe-deficient conditions. The ORF was amplified using the forward and reverse primers 5'-caccATGAGCGACGGCGGCGCAGGCTCC-3' and 5'-TCATATCTCGCCGTCCCATAGGTCGTC-3', respectively, from a cDNA library prepared from Fe-deficient rice roots. *HvDMAS1* was identified as unigene no. 6858 in the HarvEST database (Version 1.35; http://harvest.ucr.edu/) because of its strong homology to *Oryza sativa* NADPH-dependent oxidoreductase (AK073738). The *HvDMAS1* ORF was amplified using the forward and reverse primers 5'-caccATGGGCGCCGGCGATAGGACGGTCG-3' and 5'-TCATATCTCGCCGTCCCAGAGCTCCTCG-3', respectively, from a cDNA library prepared from Fe-deficient barley roots. *ZmDMAS1* and *TaDMAS1* were identified on the basis of homology using BLAST (http//:www.ncbi.nlm.nih.gov/BLAST/). Forward and reverse primers for *ZmDMAS1*

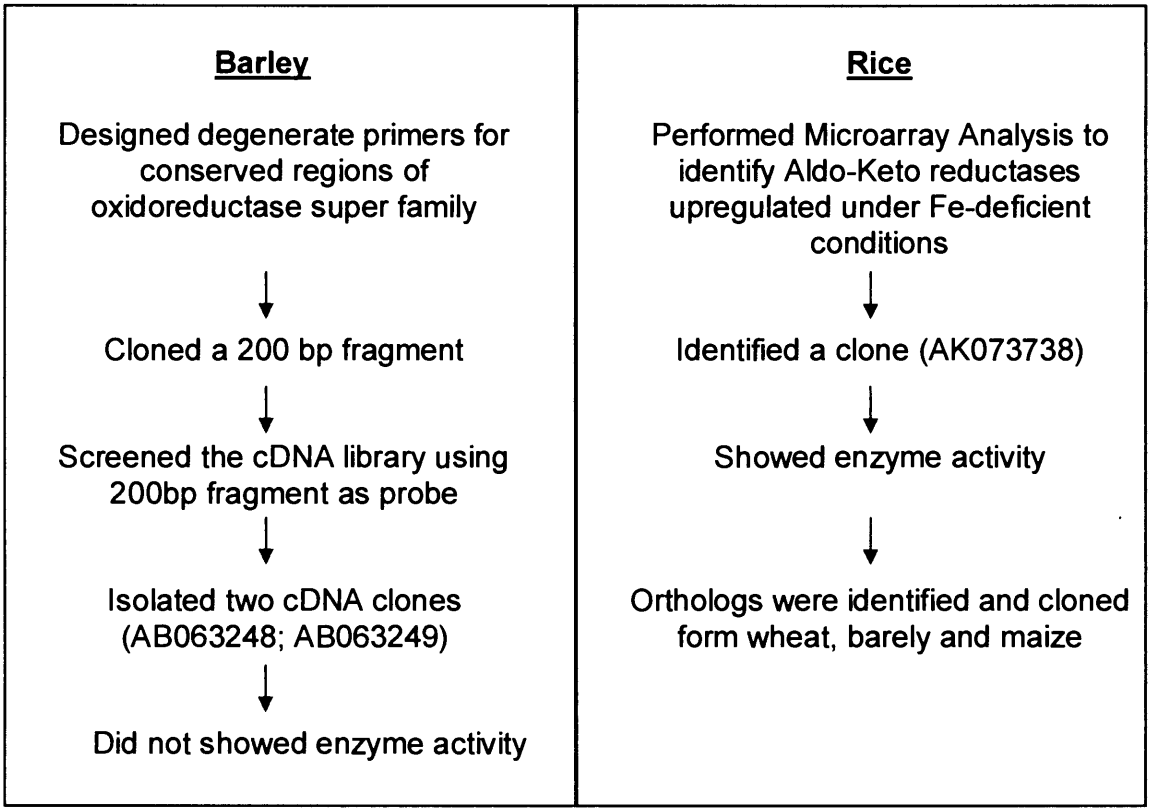

Fig-2.2: Strategies to Clone DMAS form Graminaceous Plants

were designed with the sequences 5'-caccATGAGCGCGACCGGGCGAGCCCCG-3' and 5'-TCATATCATATCTCGCCGTCCCAT-3', respectively, and the *ZmDMAS1* ORF was amplified from a cDNA library prepared from Fe-deficient maize roots. Forward and reverse primers for *TaDMAS1* were designed with the sequences 5'-caccATGGGCGCCGGCGACAAGACGG-3' and 5'-TCATATCTCGCCGTCCCAGAGCTCCTCG-3', respectively, and the ORF for *TaDMAS1* was amplified from a cDNA pool prepared from Fe-deficient wheat roots. The amplified *DMAS* cDNAs were subcloned into pENTR/D-TOPO (Invitrogen, Carlsbad, CA) and sequenced using a Thermo Sequenase Cycle Sequencing Kit (Shimadzu, Kyoto, Japan) and a DNA sequencer (DSQ-2000L; Shimadzu). The nucleotide sequences of *DMASs* were submitted to the DDBJ with accession numbers *AB269906, AB269907, AB269908* and *AB269909* for *OsDMAS1, HvDMAS1, TaDMAS1* and *ZmDMAS1* respectively. The amino acid sequences of one representative from each subfamily of the AKR family (http://www.med.upenn.edu/akr) were aligned, and the NADPH-binding domain and the putative DMAS active site were recognized as described by Jez et al., (1997). The phylogenetic relationships were determined as described (Hyndman et al., 1997).

Functional paralog of *OsDMAS1* were also searched. Members of aldo-keto reductase family in rice were identified through blast and the closest homolog of OsDMAS1, AK102609 was amplified with forward and reverse primers

5'-caccATGGCCACCATCCCGGAGGTGCCGGCG-3' and 5'-CTAGACGTCACCATCCCACAAATCTTC-3 respectively, cloned into pENTR/D-TOPO (Invitrogen, Carlsbad, CA) and sequence was confirmed as described above. Another member of AKR family, AK067910 upregulated in Fe-deficient roots was amplified with forward and reverse primers as 5'-caccATGATGGCCGGGACCCTGCAGGTCG-3 and 5'-TTACAACTTCTCTACTGGGAATCCGA-3 respectively.

In silico analysis were performed using computer program pSORT (http://psort.ims.u-tokyo.ac.jp/) to determine the subcellular localization of DMAS proteins as well as AK102609 and AK067910.

2.2.2). Protein expression and purification

Partial sequence of *HvNAAT-A* (Takahashi et al., 1999) was cloned into pET15b (Novagen) as a HisTag fusion protein and inserted into the *E. coli* strain BL21(Lys). Expression of the protein was induced and purified according to the manufacturer's instructions, and the protein was quantified using the Bradford assay (Bradford, 1976). To subclone *OsDMAS1* into pMAL-c2 (New England Biolabs, Beverly, MA), the ORF was amplified with primers to contain an *Xba*I site at the 5' end and a *Hin*dIII site at the 3' end. The ORF was amplified, subcloned into pCR-BluntII-TOPO (Invitrogen, Carlsbad, CA), and sequenced. The resulting plasmid was then digested with *Xba*I and *Hin*dIII and the excised fragment containing *OsDMAS1* was subcloned into pMAL-c2. This plasmid was designated

pMAL-c2-*OsDMAS1*. *HvDMAS1*, *TaDMAS1*, *ZmDMAS1*, AK102609 and AK067910 were also subcloned into pMAL-c2 in the same manner. These pMAL-c2 plasmids were introduced into *E. coli* XL1-Blue, the cells were induced to produce the recombinant fusion proteins, and the recombinant proteins were purified as described (Higuchi et al., 1999).

2.2.3). Enzyme assay

Five μg of HvNAAT-A fusion protein/reaction were centrifuged in an Amicon Ultrafree-MC 30-kDa-cutoff filter unit (Millipore) at 6200 × *g* at 4 °C for 15 min. The flow-through was discarded, and 50 μl of N-[Tris(hydroxymethyl)methyl]-3-aminopropane-sulfonic acid buffer (50 mM TAPS, 5 mM KCl, 5 mM $MgCl_2$, 10 mM 2-oxoglutaric acid, 10 μM pyridoxal-5'-phosphate (PLP), 150 μM NA) was added to the filter unit. The solution was mixed several times by pipetting and incubated at 26°C for 30 min. The filter unit was then placed in a new Eppendorf tube and centrifuged at 6200 × *g* at 4°C for 15 min. The flow-through was collected and NADPH was added to a final concentration of 25 μM. The protein samples to be assayed (1 μg/reaction) were placed in new filter units and centrifuged at 6200 × *g* at 4°C for 1 min. All of the samples were prepared separately, including a chemical control ($NaBH_4$) and a negative control (AK102609/AK067910 bound to maltose binding protein). Then, 46 μl of flow-through containing the 3"-keto intermediate and NADPH, prepared as described above, were added to each filter unit containing DMAS, mixed two to

three times by pipetting, and incubated at 26°C for 30 min. For the chemical control, 4 µl of 0.25 M $NaBH_4$ were added, and the mixture was centrifuged for 1 min and held at 26°C for 5 min. The filter units were then placed in new Eppendorf tubes and the flow-through were collected by centrifugation at 6200 × *g* at 4°C for 5 min. Then, 50 µl of each sample was analyzed by HPLC using 5 µ mole of purified DMA as a standard. All reactions were performed in duplicate.

To perform enzyme assays at pH 7, 8, and 9, NA was first converted to the 3"-keto intermediate as described above, the pH of the flow-through was adjusted to 7 or 8 with Tris-Cl buffer (pH 1.1) or diluted with TAPS buffer at pH 8 or 9 (**Table-1** and **Fig-2.3**), and the samples were processed as described above. All reactions were performed in triplicate.

2.2.4). Northern blot analysis

Seeds of barley (*Hordeum vulgare* L. cv. Ehimehadaka no. 1), wheat (*Triticum aestivum* L. cv. Chinese spring), maize (*Zea mays* cv. Alice), and rice (*Oryza sativa* L. cv. Nipponbare) were germinated on wet filter paper and cultured as described (Kanazawa et al., 1994). For Fe-deficiency treatments, plants were transferred to culture solution lacking Fe. Roots and leaves were harvested after two weeks, frozen in liquid nitrogen, and stored at -80°C until use.

Total RNA was extracted from roots and shoots, and 10 µg per lane were electrophoresed in 1.2% (w/v) agarose gels containing 0.66 M formaldehyde and transferred to Hybond-N+ membrane (Amersham, USA). The *HvDMAS1* ORF was

labeled with digoxigenin (DIG) and incubated with the membrane at 68°C and processed as described (Engler Blum et al., 1993; Yoshihara et al., 2003).

2.2.5). Western Blot Analysis

Proteins were extracted as described in **section-3.2.3** from Fe-deficient and Fe-sufficient rice, barley, maize and wheat root and shoots. 10 µg of total protein was separated using SDS-PAGE, and blotted as described previously (Higuchi et al. 1999). The polyclonal DMAS antibodies were used for Western-blot analysis, along with a secondary antibody, goat anti-mouse IgG (H+L) conjugated with horseradish peroxidase (Wako, Osaka, Japan). Then blotting membrane was stained with diaminobenzidine.

Table-1: Adjustment of pH for Enzyme Assay

	Volumes (µl)			
pH	**Buffer containg 3"-keto intermediate**	**Tris-Cl (pH 1.1)**	**Taps Buffer**	**Final**
7	270	108	0	378
8	270	49	59	378
9	270	0	108	378

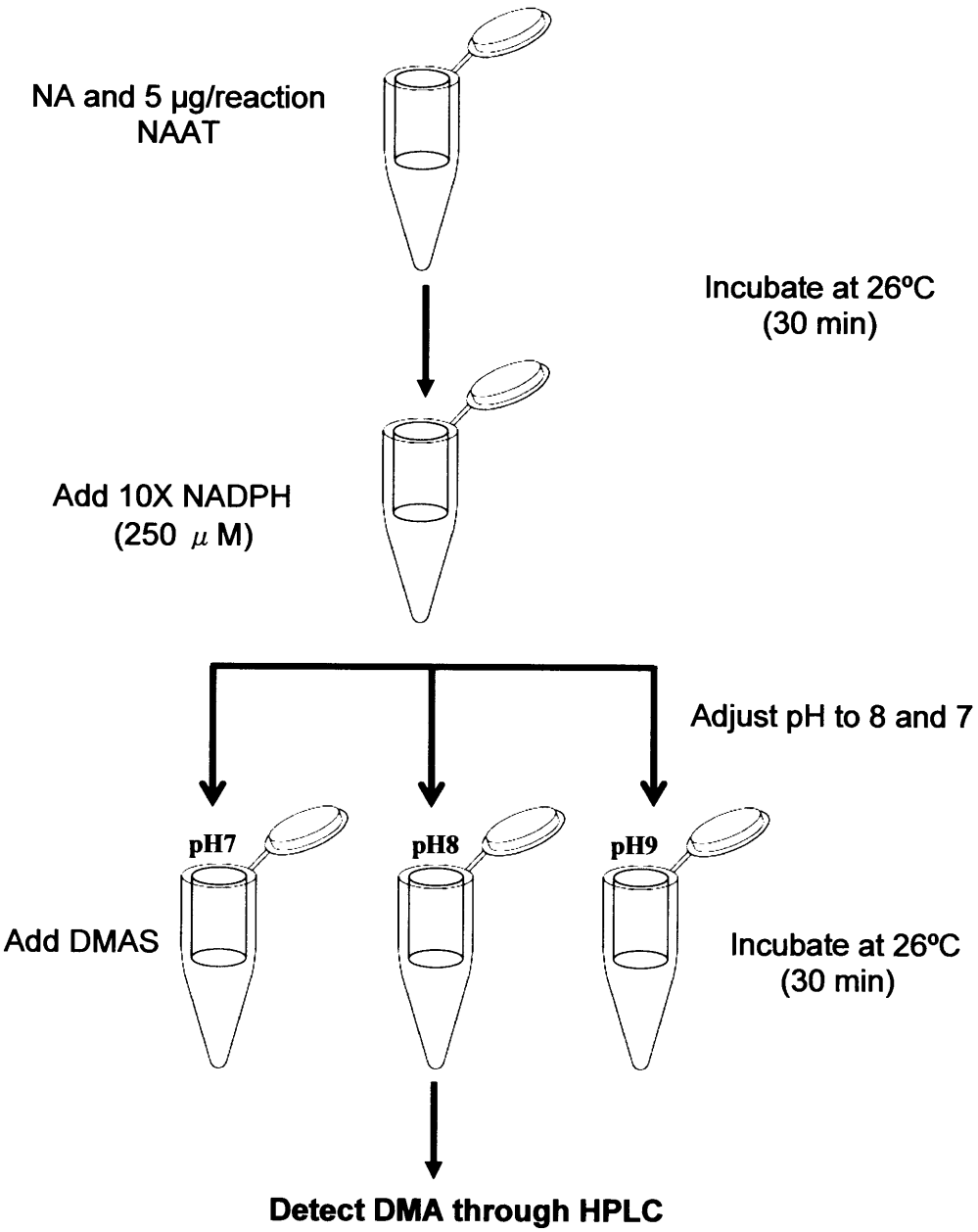

Fig-2.3: Adjustment of pH for Enzyme Assay at pH 7, 8 and 9

2.3). Results

2.3.1). Isolation of *DMAS* genes

OsDMAS1 (AK073738: NAD(P)H dependent oxidoreductase) was identified as a putative member of the aldo-keto reductase superfamily, upregulated under Fe-deficient conditions. *OsDMAS1* is located on rice chromosome 3 and is composed of four exons and three introns (**Fig-2.4a**). The length of the genomic fragment is 2706 bp, and that of the ORF is 957 bp. The promoter region of the gene contains Fe-deficiency responsive element 2 (IDE2)-like sequence (Kobayashi et al., 2003; Kobayashi et al., 2005). *OsDMAS1* shows 54.7% homology to *Papaver somniferum* codeinone reductase (AKR4B2-3) and 48 and 50% homology to *Medicago sativa* and *Glycine max* chalcone polyketide reductase (AKR4A2 and AKR4A1), respectively. AKR have 15 families (AKR1-AKR15) (Yokochi et al., 2004) and the criteria for classification of AKR is that members within a family have less than 40% amino acid sequence identity with other families and that members within a subfamily have greater than 60% sequence identity (Hyndman et al., 2003). Based on this criterion, DMAS proteins do not fall in existing subfamilies of AKR4 (**Fig-2.4b**). The sequence of DMAS was submitted to AKR database maintained at http://www.med.upenn.edu/akr/ (Hyndman et al., 2003). After introduction of conservative substitutions, the identity with existing members of AKR4B reached up to 65% and ZmDMAS1, OsDMAS1, HvDMAS1 and TaDMAS1 were assigned the numbers from AKR4B5 to AKR4B8 respectively. The full-length *HvDMAS1* was identified as unigene no. 6858 in the

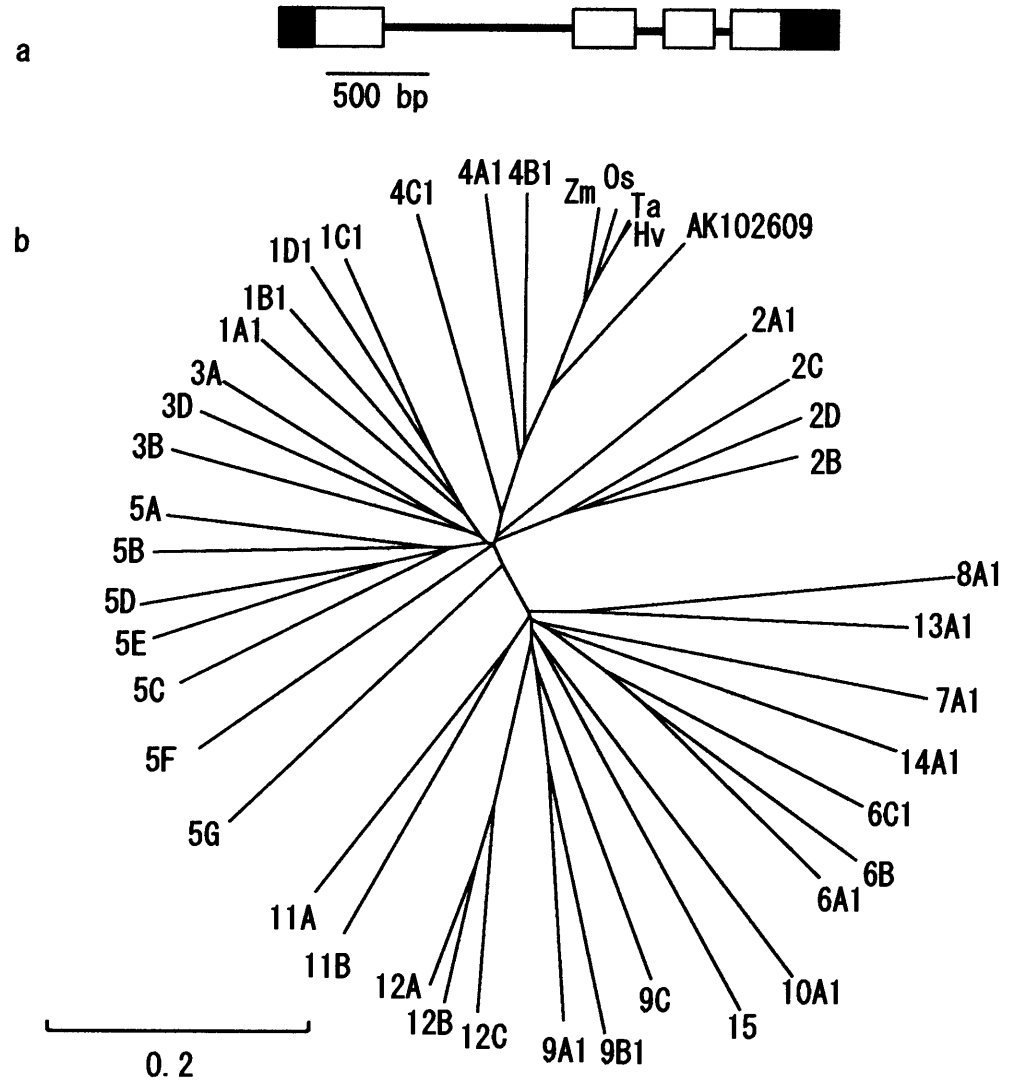

Fig-2.4: Structural and Phylogenetic Characterization of *DMAS* Genes

a) Genomic structure of *OsDMAS1*. *OsDMAS1* is composed of four exons (boxes) and three introns. Black boxes indicate 5'- and 3'-UTRs.

b) Unrooted phylogenetic tree of the aldo-keto reductase superfamily (AKR). The details and accession numbers of the AKR proteins are at http://www.med.upenn.edu/akr/members.html. Accession numbers of DMASs are as OsDMAS1: AB269906; HvDMAS1: AB269907; TaDMAS1: AB269908; ZmDMAS1: AB269909. AK102609 is a homolog of OsDMAS1 that lacks DMAS activity.

HarvEST database (Version 1.35; http://harvest.ucr.edu/) and is homologous to rice NADPH-dependent oxidoreductase. *OsDMAS1* and *HvDMAS1* show 86% homology. *TaDMAS1* and *ZmDMAS1* were identified by BLAST on the basis of homology. All four *DMAS* orthologs were isolated from cDNA libraries prepared from Fe-deficient roots. The nucleotide sequences show that *OsDMAS1* encodes a predicted polypeptide of 318 amino acids, and the other three *DMAS* clones each encode predicted polypeptides of 314 amino acids (**Fig-2.5**).

The DMAS sequences from graminaceous plants are highly conserved (82 to 97.5%). HvDMAS1 and TaDMAS1 show the greatest homology (97.5%). All of the DMAS proteins possess the NADPH-binding domain, as do all other AKRs. The active-site sequences in these proteins are strictly conserved, although in ZmDMAS1 the Lys is replaced with Thr at position 123 (**Fig-2.5**). Rice contains a number of AKR family members (**Fig-2.6a**) but expression of only a few is regulated by Fe (**Table-2**). The closest homolog of OsDMAS1 in rice, AK102609 is located on rice chromosome 10 and is split in to 2 exons (**Fig-2.6b**). The length of the genomic fragment is 2.173kb and it is predicted to encode a polypeptide of 322 amino acids. Another clone AK067910 regulated by Fe-deficiency is located on rice chromosome 7 and predicted to encode a polypeptide of 377 amino acids. The genomic structure of AK067910 is composed of 10 exons separated by 9 introns (**Fig-2.6c**). The length of genomic fragment encoding AK067910 is 3.844 kb. The subcellular localization of DMAS proteins was predicted with compute software pSORT (http://psort.ims.u-tokyo.ac.jp/). The OsDMAS1 and HvDMAS1 were

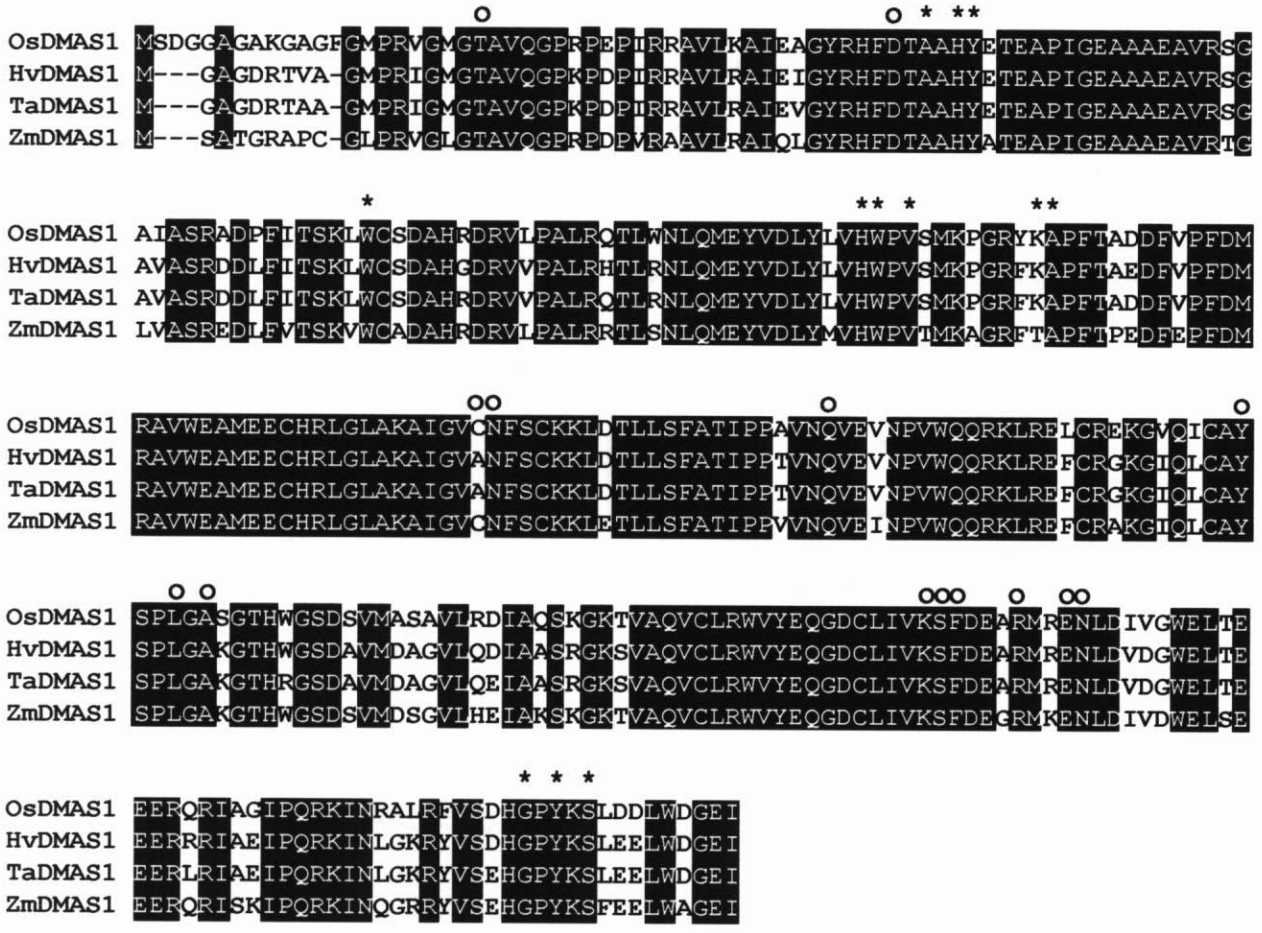

Fig-2.5: Sequence Similarities between Graminaceous DMAS Proteins

An alignment of the deduced amino acid sequences of the proteins encoded by OsDMAS1, HvDMAS1, TaDMAS1, and ZmDMAS1 is shown. The identities between the four orthologs are indicated by black boxes. Circles and asterisks above the alignment indicate the putative NADPH-binding domain and the putative substrate-binding domain, respectively.

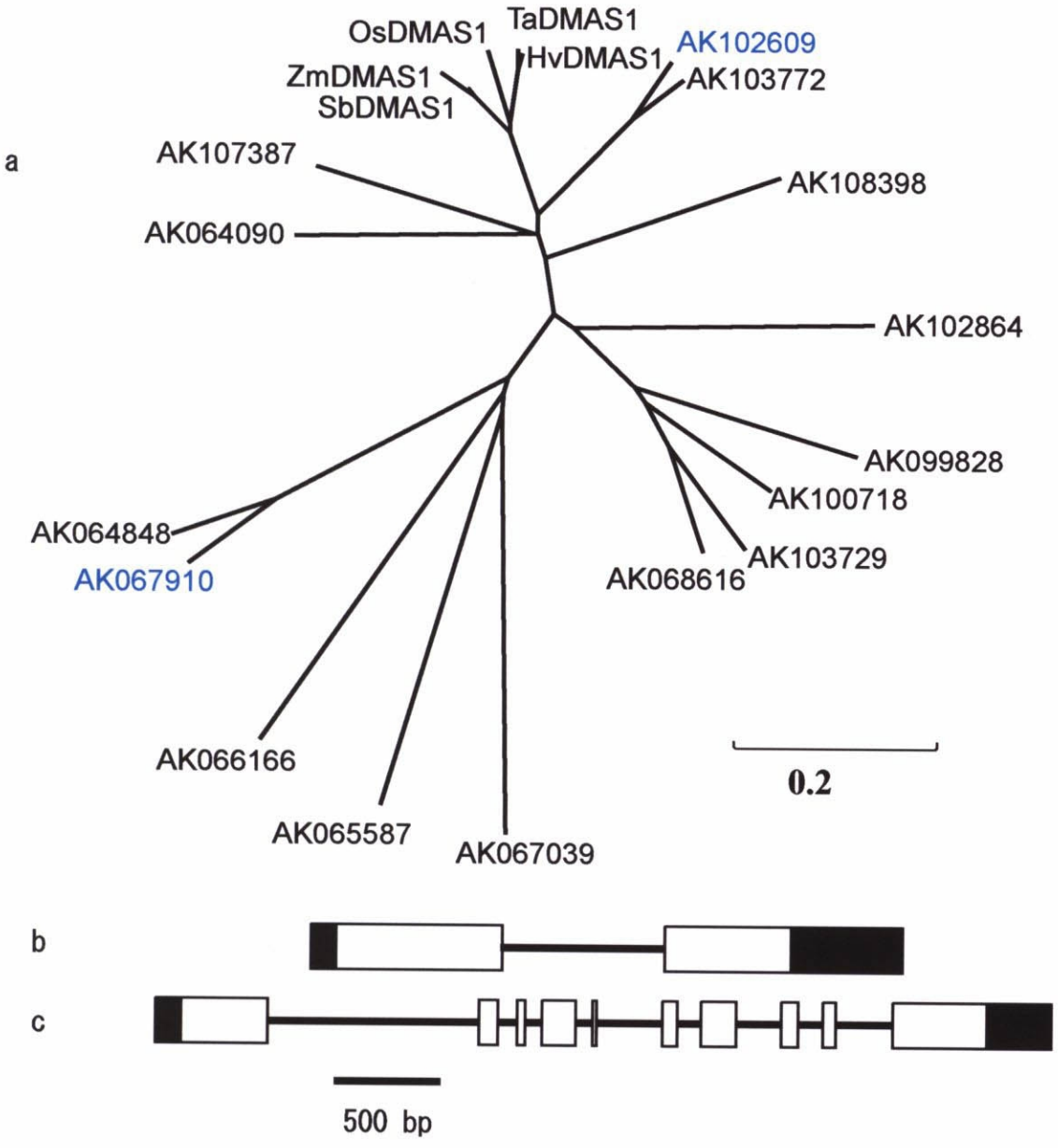

Fig-2.6: Putative Members of AKR Family in Rice

a) Phylogenetic tree of the AKR members in rice. Predicted full length proteins were used to generate phylogenetic tree.
b) Genomic structure of AK102609. AK102609 is composed of two exons (boxes) and one intron. Black boxes indicate 5'- and 3'-UTRs.
c) Genomic structure of AK067910. AK067910 is composed of 10 exons (boxes) and nine introns. Black boxes indicate 5'- and 3'-UTRs.

Table-2: Members of Aldo-Keto Reductase Super Family Induced Under Fe-deficient Conditions

AK Number	New Leaf	Old Leaf	Root
AK073738 (*OsDMAS1*)	4.4	2.0	4.6
AK102609	3.2	2.1	0.4*
AK067039	1.4	2.2	1.3*
AK067910	0.9	1.0	6.4

*: Did not showed enzyme activity

predicted to be localized to micro bodies while TaDMAS1, ZmDMAS1, AK102609 and AK067910 were predicted to be localized to cytoplasm (**Table-3**).

2.3.2). Enzyme assay

The *DMAS* cDNAs from rice, barley, wheat, and maize were expressed in *E. coli*, and size was confirmed by SDS page analysis (**Fig-2.7**). The expressed proteins were tested for the ability to convert the 3"-keto intermediate into DMA. As the 3"-keto intermediate could not be chemically synthesized, it was necessary to use an *in vitro* enzyme assay that begins with NA. In this assay, NA is first converted into the 3"-keto intermediate by the action of HvNAAT-A and is subsequently converted into DMA, which is identified through HPLC (**Fig-2.8**). *In vitro*, all four proteins were able to convert the 3"-keto intermediate into DMA (**Fig-2.9**). However the AK102609 and AK067910 did not showed enzyme activity. The highest enzyme activity was observed for TaDMAS1, followed by OsDMAS1, ZmDMAS1, and HvDMAS1 (**Fig-2.9 & 2.10**).

The effect of pH on enzyme activity was also examined. Enzyme assays were performed at pH 7, 8, and 9 (**Fig-2.10**). At pH 7, the enzyme activities were 6.5 to 14.9 times lower than those at pH 8, but the enzyme activities at pH 8 and 9 were comparable. The DMA synthesis by $NaBH_4$ at pH 7 also decreased. However this difference was negligible as compared with reduction in DMA synthesized by graminaceous DMASs. These results strengthen the hypothesis that DMA is synthesized in subcellular vesicles derived from rough ER, as the DMAS activities were much lower at the neutral pH of the cytoplasm.

Table-3: Predicted Subcellular Localization of DMASs

Clone	Subcellular Localization	Probability
OsDMAS1	Microbody (peroxisome)	= 0.498
	Cytoplasm	= 0.450
HvDMAS1	Microbody (peroxisome)	= 0.487
	Cytoplasm	= 0.450
TaDMAS1	Cytoplasm	= 0.450
	Microbody (peroxisome)	= 0.403
ZmDMAS1	Cytoplasm	= 0.450
	Microbody (peroxisome)	= 0.232
AK102609	Cytoplasm	= 0.450
	Chloroplast (Stroma)	= 0.200
AK067910	Cytoplasm	= 0.450
	Microbody (peroxisome)	= 0.370

The subcellular localization was determined with the help of computer program, PSORT at (http://psort.ims.u-tokyo.ac.jp/)

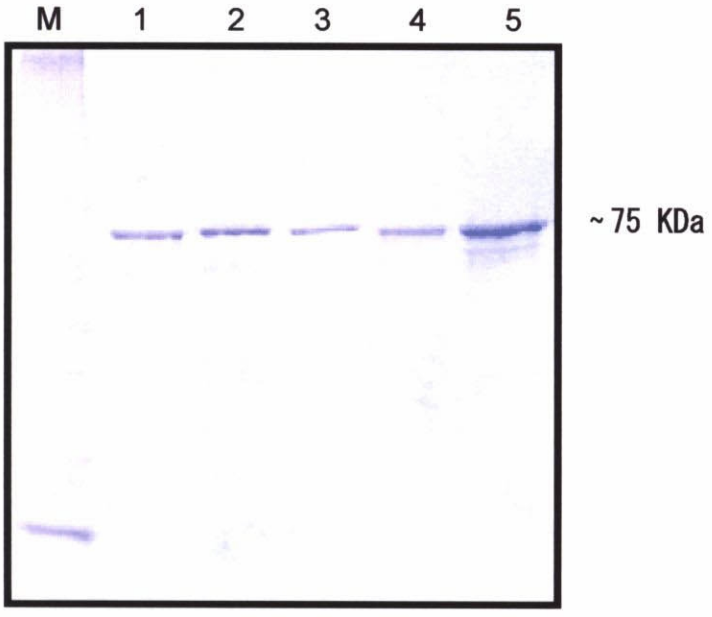

Figure-2.7. SDS PAGE of Recombinat DMASs Proteins

M: Marker; 1: OsDMAS1; 2:HvDMAS1;
3:TaDMAS1; 4:ZmDMAS1; 5: AK102609

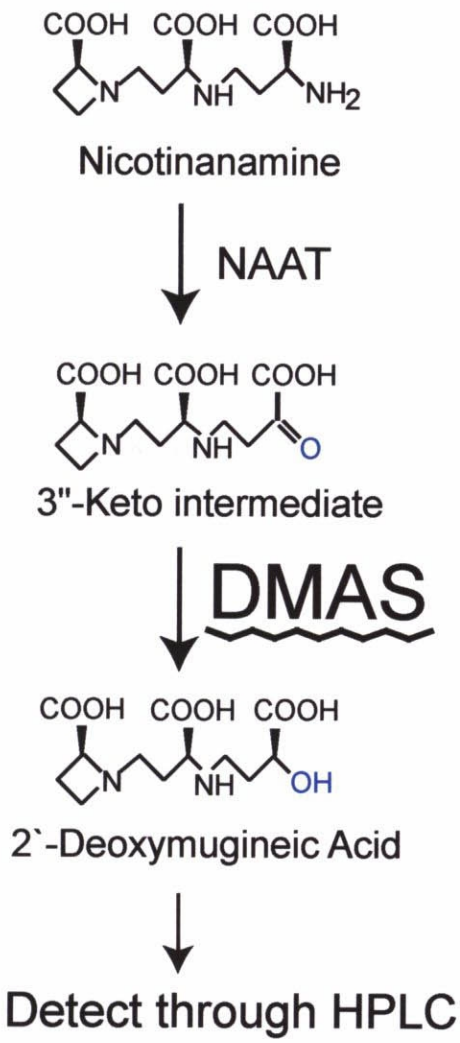

Fig-2.8: Schematic Diagram of Enzymy Assay for DMAS Activity

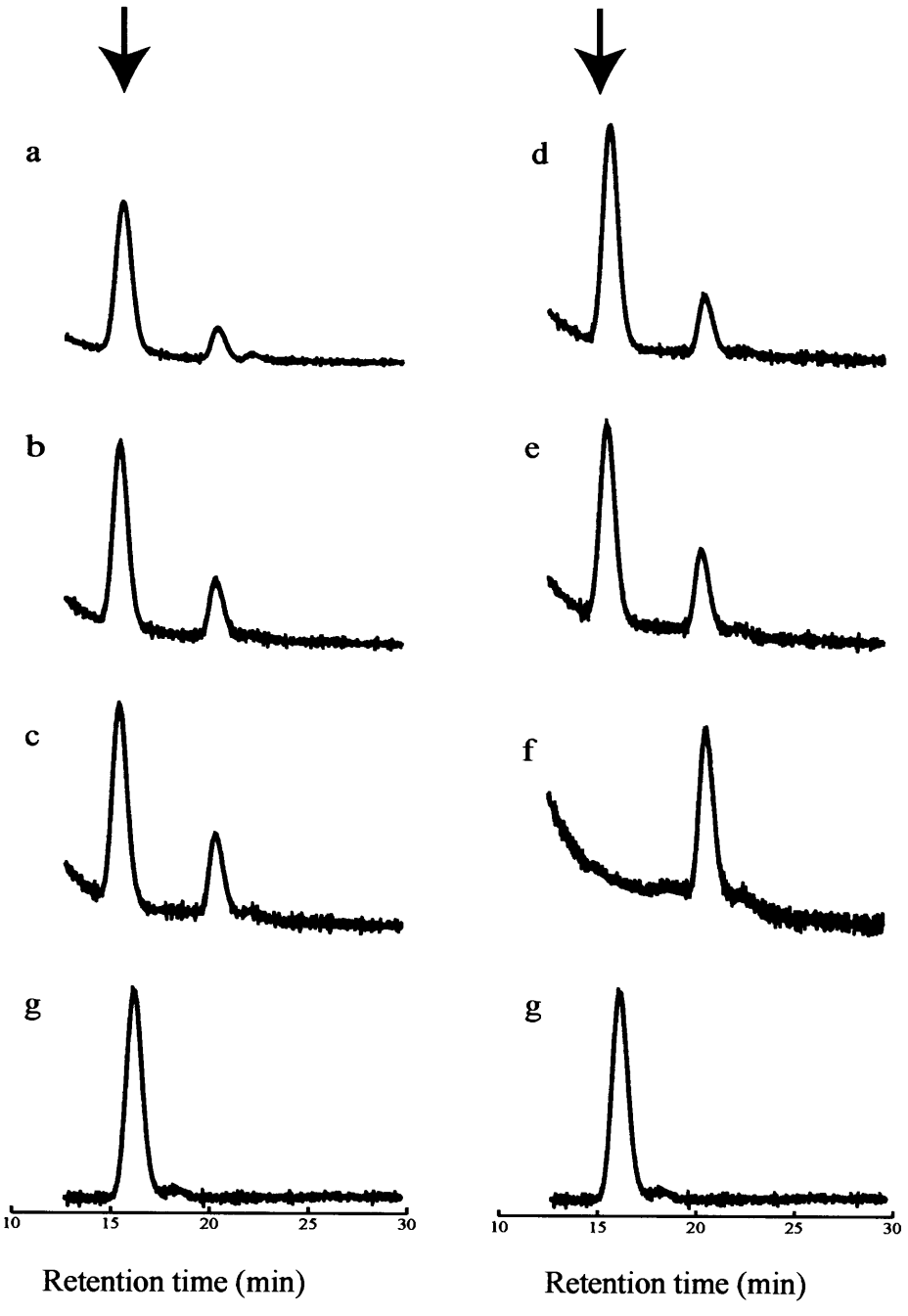

Fig-2.9: HPLC Profiles of Enzymatic Activity of DMAS Proteins

Enzyme activity was determined by the detection of DMA in HPLC using DMA as a standard. Reduction by a) NaBH4, b) OsDMAS1, c) HvDMAS1, d) TaDMAS1, e) ZmDMAS1, f) negative control (AK102609 or AK067910), and g) purified DMA are shown. The peaks corresponding to DMA are indicated by arrows.

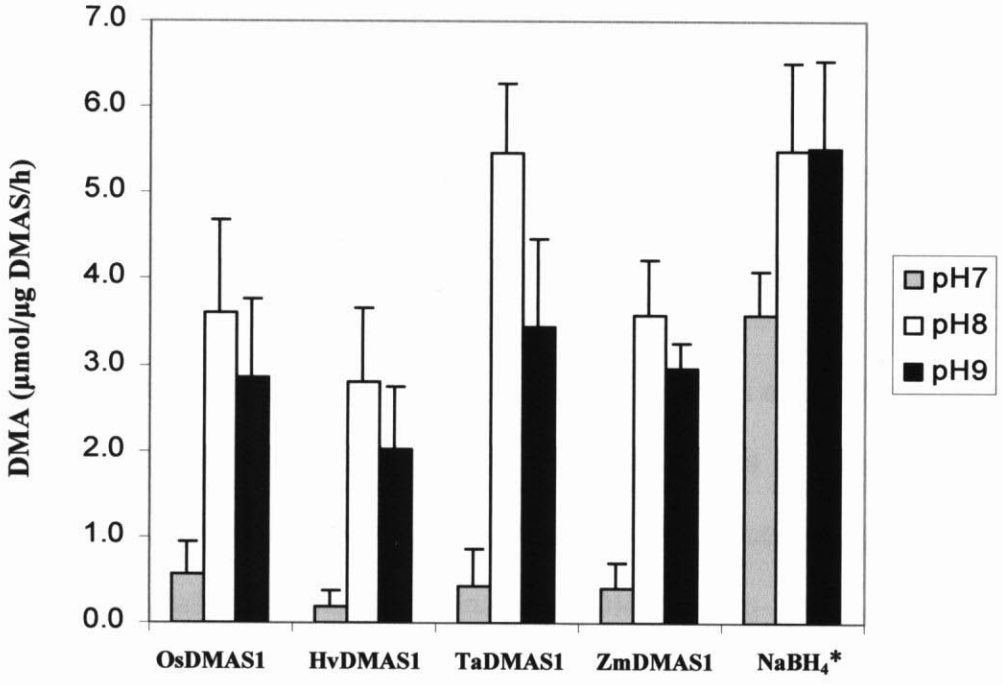

Fig-2.10: Effect of pH on Enzyme Activity of DMAS

In vitro enzyme assays were performed at pH 7, 8, and 9. DMAS specific activity is expressed as the mean ± standard deviation of triplicate assays.

* For $NaBH_4$ DMA was synthesized by 20 mM $NaBH_4$.

2.3.3). Northern blot analysis

OsDMAS1 was identified as a gene that is upregulated under Fe-deficient conditions. The expression pattern was further characterized by Northern blot analysis, which revealed that under Fe-deficient conditions, the expression of all of the *DMAS* genes is upregulated in root tissue, but only the expression of *OsDMAS1* and *TaDMAS1* is upregulated in shoot tissue (**Fig-2.11a**). The expression of DMAS was high in barley while it was low in rice and maize. As *HvDMAS1* ORF was used as probe so there were chances that low expression may be due to the reason that *HvDMAS1* does not recognize *OsDMAS1* and *ZmDMAS1* with equal efficiency as compared with *HvDMAS1* and *TaDMAS1*. To resolve this problem plasmid southern analysis were performed which revealed that probe prepared from *HvDMAS1* ORF equally recognized graminaceous DMASs (**Fig-2.11b**).

2.3.4). Western blot analysis

Western Blot analysis revealed that the expression of DMAS is upregulated in response to Fe-deficiency in roots of rice, wheat and barley (**Fig-2.12**). Under Fe-sufficient conditions the expression was only observed roots of wheat. No expression was observed in Fe-sufficient or deficient leaves of rice, wheat, barley or maize. This may be due to low expression of DMAS in shoot tissue. No band was observed in maize either in root or shoot or even under Fe-deficient conditions. This may also be due to low expression of DMAS in maize.

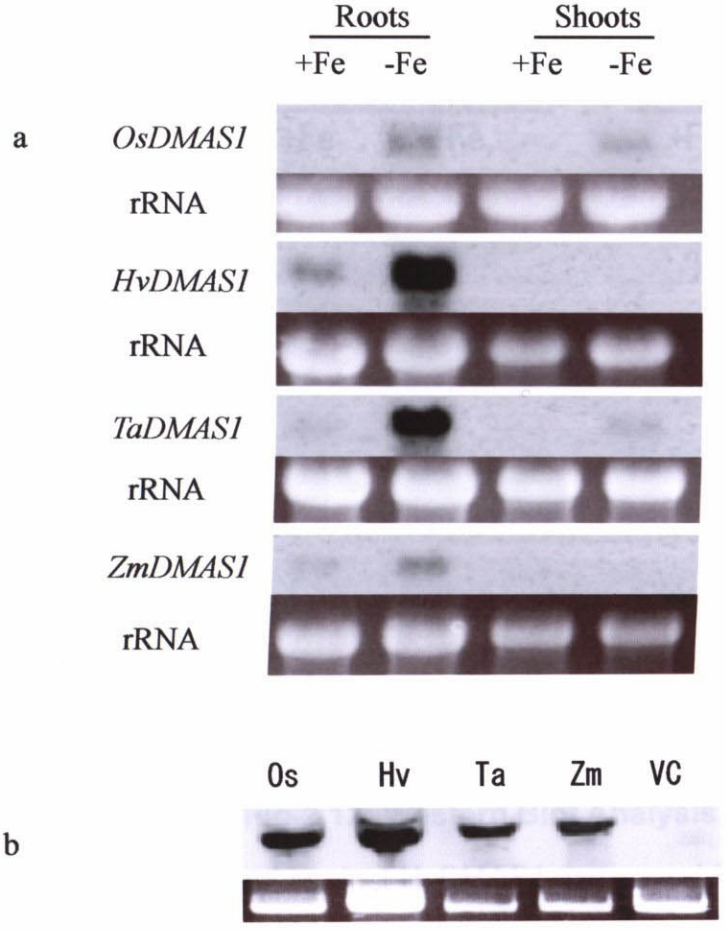

Fig-2.11: Northern Blot Analysis of DMAS

a) Northern blot analysis of graminaceous DMAS. Full length ORF of *HvDMAS1* was used as probe.

b) Plasmid southern blot analysis.
pMALc2 containing respective DMAS was digested with *Xba*I and *Hind*III and used for plasmid southern analysis. Full length ORF of HvDMAS was used as probe.

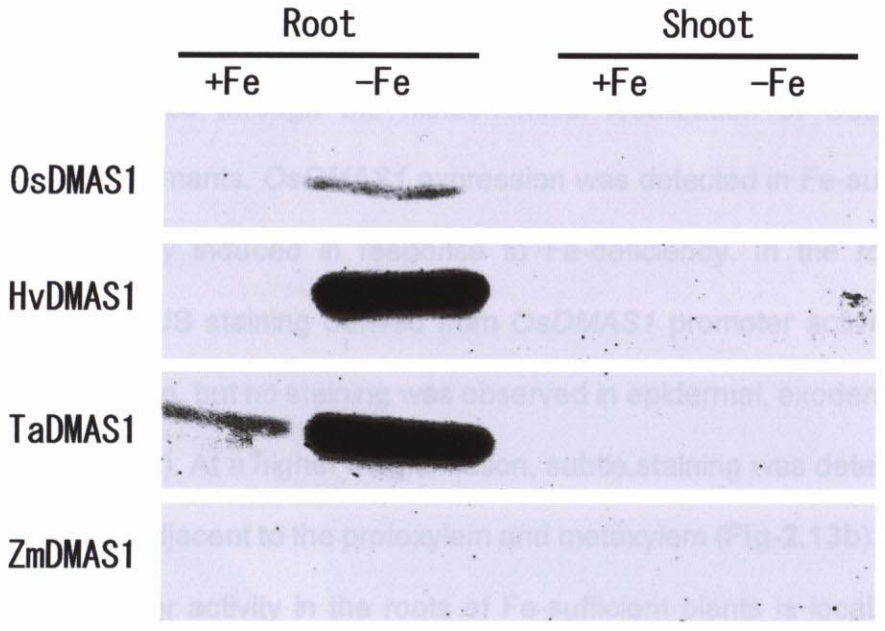

Fig-2.12: Western Blot Analysis of DMAS

Antibodies rasied against HvDMAS1 were used for Western blot analysis.

2.3.5). Spatial pattern of *OsDMAS1* expression

To gain a more detailed insight into the physiological roles of the *OsDMAS1* gene, the localization of its expression in both Fe-sufficient and Fe-deficient rice plants were investigated through the histochemical localization of *OsDMAS1* promoter-*GUS* transformants. *OsDMAS1* expression was detected in Fe-sufficient roots and was strongly induced in response to Fe-deficiency. In the roots of Fe-sufficient plants, GUS staining derived from *OsDMAS1* promoter activity was observed within the stele, but no staining was observed in epidermal, exodermal, or cortical cells (**Fig-2.13a**). At a higher magnification, subtle staining was detected in part of pericycle cells adjacent to the protoxylem and metaxylem (**Fig-2.13b**). Thus, the *OsDMAS1* promoter activity in the roots of Fe-sufficient plants is localized in cells that participate in long-distance transport. Longitudinal sections of Fe-sufficient roots showed no GUS staining (**Fig-2.13c**).

In roots of Fe-deficient plants, the *OsDMAS1* promoter was active in all tissues, including the epidermis, exodermis, cortex, and whole stele (**Fig-2.13e**). Particularly staining was observed in pericycle cells adjacent to the protoxylem and metaxylem I (**Fig-2.13f**), as was evident in Fe-sufficient roots. Interestingly, GUS activity was detected in cells surrounding the metaxylem I, in both Fe-sufficient and Fe-deficient roots, in the region from which lateral roots emerge. No GUS expression was detected in leaves of Fe-sufficient plants (**Fig-2.13g**), whereas under Fe-deficient conditions GUS activity was detected in phloem, parenchyma and companion cells (**Fig-2.13h**).

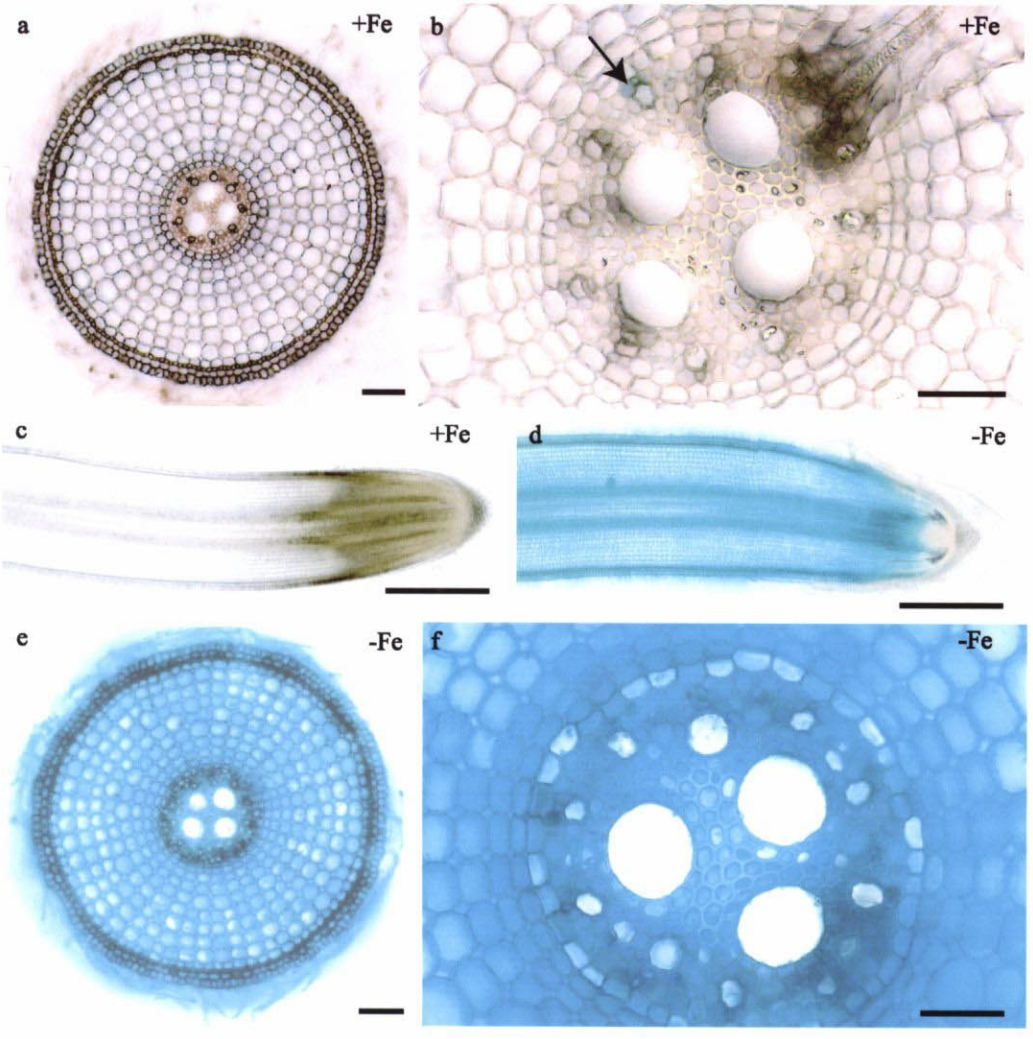

Fig-2.13: Histochemical Localization of OsDMAS1 Promoter Activity in Promoter-GUS Transgenic Plants Cultured Hydroponically Under Fee-sufficient (+Fe) or Fe-deficient (-Fe) Conditions.

a (+Fe), e (-Fe): root transverse section; b (+Fe), f (-Fe): enlarged part of stele; c) (+Fe), d (-Fe): root longitudinal section; g (+Fe), h (-Fe): longitudinal section of leaf tissue.
Scale: 500 µm (c, d); 100 µm (a, e); 50 µm (b, f, g, h).

2.4). Discussion

The biosynthetic pathway for MAs has been characterized (**Fig-2.1**) in extensive physiological and biochemical studies (Mori and Nishizawa, 1987; Ma et al., 1995; Kawai et al., 1988; Shojima et al., 1990). It was proposed that the 3"-keto intermediate is converted to DMA by the action of the enzyme DMAS (Nomoto et al., 1987). All of the genes involved in the DMA biosynthetic pathway have been reported as being isolated, with the exception of *DMAS*. It was reported (Shojima et al., 1990) that DMAS activity is dependent on NAD(P)H, raising the possibility that *DMAS* is a member of the AKRs. The AKRs (Nelson et al., 1986) comprise one of the three enzyme super families that encompass NAD(P)(H)-dependent oxidoreductases (Hyndman et al., 1997) and catalyze the reduction of aldehydes, ketones, monosaccharides, ketosteroids, and prostaglandins. This superfamily contains more than 120 enzymes, which are divided into 15 families (AKR1-AKR15) (Yokochi et al., 2004), nine of which contain multiple subfamilies (Hyndman et al., 1997). These proteins possess the $(\alpha/\beta)_8$ barrel motif, which provides a common scaffold for NAD(P)(H)-dependent catalytic activity, with the substrate specificity determined by variations in loops on the C-terminal side of the barrel (Jez et al., 1997). The NADPH-binding domain is conserved, even in proteins with less than 30% homology (Jez et al., 1997). The majority of known AKRs are monomeric proteins of about 320 amino acids in length, but multimeric forms also exist (Hyndman et al., 1997). AKRs have been well characterized, with three-dimensional structures elucidated for many (Jez et al., 1997). However, few

AKRs from graminaceous crops have been characterized. The isolation and characterization of *DMAS* genes from rice, barley, wheat, and maize is an important step in the characterization of the AKRs. According to the database of aldo-keto reductase super family (http://www.med.upenn.edu/akr/) it is the first member of AKR family cloned from rice and wheat. *OsDMAS1* encodes a protein of 318 amino acids that can be considered a model for the structures of other DMASs. Although there is some variation among graminaceous DMASs, the substrate-binding domain is strictly conserved (**Fig-2.5**). The replacement of Lys by Thr at position 123 in ZmDMAS (**Fig-2.5**) has no effect on enzyme activity (**Fig-2.9**). The role of the amino acid at this position in substrate recognition is not well understood (Jez et al., 1997). The NADPH-binding domain is also conserved, which is a striking feature of the AKRs. An alignment of the sequences of known AKR members revealed that DMASs belong to the AKR4 group and show homology to *P. somniferum* codeinone reductase (AKR4B2-3) and *Medicago sativa* (AKR4A2) and *Glycine max* (AKR4A1) chalcone polyketide reductases. Strictly speaking it does not fall into existing subfamilies of AKR4, however, after introduction of conservative substitutions, the identity with existing members of AKR4B reached up to 65% and ZmDMAS1, OsDMAS1, HvDMAS1 and TaDMAS1 were assigned the numbers from AKR4B5 to AKR4B8 respectively. On the base of substrate specificity DMAS define a novel class of reductases.

With the isolation of graminaceous *DMAS* genes, the genes encoding all of the enzymes involved in the biosynthetic pathway of MAs have been isolated,

including S-adenosylmethionine synthetase (*SAMS*) (Takizawa et al., 1996), *NAS* (Higuchi et al., 1999), *NAAT* (Takahashi et al., 1999), *IDS*2, and *IDS*3 (Nakanishi et al., 2000). Moreover, it was proved that 3"-keto acid is an intermediate in the pathway from NA to DMA. All of the DMAS proteins were able to synthesize DMA from the 3"-keto intermediate *in vitro* (**Fig-2.9, 2.10**). *TaDMAS1* showed the highest enzymatic activity, and barley secretes the greatest amounts of MAs (Römheld et al., 1990; Singh et al., 1993). In rice roots, the amount of NA is higher and the amount of DMA is lower than in barley roots (Higuchi et al., 2001), suggesting that *HvDMAS1* is more active and utilizes more NA for DMA production. Interestingly, the endogenous NAS activity is also higher in wheat than in barley (Higuchi et al., 1999). DMASs appear more active than NAAT, as five µg of NAAT protein were used for each reaction, as compared to 1 µg of each DMAS, and still it seems that the 3"-keto intermediate is a limiting factor for *TaDMAS1* and the chemical control (**Fig-2.10**). The reduction at the 3"-carbon of the 3"-keto intermediate by $NaBH_4$ is not thought to be sterically specific, as in the case of enzymatic reduction, and not all of the chemically produced DMA may have the same three-dimensional structure as natural DMA at the 3"-carbon (Ohata et al., 1993). The enzymatic activity of these proteins was severely restricted at cytoplasmic pH, suggesting that the enzyme localizes to some subcellular organelle(s) with high pH. Although the synthesis of DMA by $NaBH_4$ also decreased at pH 7 but the difference was far less as compared DMA synthesized by graminaceous DMASs. It may be due to the reason that although $NaBH_4$ is not stable in water but it is comparatively stable in

alkaline conditions. So the difference in reduction by $NaBH_4$ at pH 7 and 8-9 is due to the decrease in available active $NaBH_4$, although enough amount of $NaBH_4$ was added to the reaction. Therefore the possibility that at pH 7 the $NaBH_4$ itself is limiting factor for the synthesis of DMA cannot be excluded. On the other hand the 3"-keto intermediate is stable at pH 7. Moreover the difference of synthesized DMA by $NaBH_4$ at pH 7 and 8-9 is far less (about 0.4 time different) as compared with the difference observed for DMASs at pH 7 and 8-9 (6.5 to 14.5 times different). The optimum pH for NAS is 9 (Higuchi et al., 1995), whereas for NAAT it is 8.5 (Ohata et al., 1993) to 9 (Shojima et al., 1990). MAs are thought to be synthesized in root tissue in vesicles derived from rough ER (Mori and Nishizawa, 1987). These vesicles remain swollen until the onset of MA secretion, and become shrunken by the end of secretion (Mori and Nishizawa, 1987). The polar transport of these vesicles has been implicated in phytosiderophore secretion in Fe-deficient barley roots (Negishi et al., 2002, Nozoe et al., 2004). NAS and NAAT are thought to be localized to these vesicles. The optimum pH for DMAS activity suggests that the DMAS protein may localize to these subcellular vesicles where DMA is synthesized and stored until secretion. However *in silico* analysis did not supported this hypothesis. Although AKRs have been reported to be active at pHs from 6.8 to 11 (Yokochi et al., 2004), AKR4 proteins have an optimal pH around 7, as has been determined for *H. vulgare* aldehyde reductase, *P. somniferum* codeinone reductase, and *Digitalis purpurea* aldose reductase (Roncarati et al., 1995; Unterlinner et al., 1999; Gavidia et al., 2002). More than one gene exists for *HvNAS* (Higuchi et al.,

1999, Herbick et al., 1999), *OsNAS* (Inoue et al., 2003), *HvNAAT* (Takahashi et al., 1999), and *OsNAAT* (Inoue et al., unpublished data), which raises the possibility that more than one *DMAS* gene exists. However the rice genes, AK102609 (a probable NADPH-dependent oxidoreductase 1) closest homolog of OsDMAS1 (63% identity), and AK067910 did not show DMAS activity (data not shown).

MAs are secreted in the morning in a distinct diurnal rhythm (Takagi et al., 1984), and the genes involved in MA biosynthesis are also expressed in a diurnal fashion (Negishi et al., 2002, Nozoe et al., 2004). The promoter region of *OsDMAS1* contains *cis*-acting elements, including an IDE2-like sequence (Kobayashi et al., 2003, Kobayashi et al., 2005), (-1408 to -1434) and evening elements (Harmer et al., 2000; Nozoe et al., 2004), (-262 to -201; -667 to -734; -702 to -752; EE: AATATCT), suggesting that its expression is regulated by Fe-deficiency in a diurnal fashion. Like all other genes involved in the MA biosynthetic pathway, *DMAS* genes are upregulated under Fe-deficient conditions in root tissue. In Fe-deficient shoots, *DMAS* expression was upregulated in rice and wheat, whereas no expression was detected in barley and maize (**Fig-2.11**). Interestingly, in rice, most of the genes involved in the MA biosynthetic pathway are expressed in both root and shoot tissues, but the expression of these genes is restricted to root tissue in barley, the graminaceous plant most tolerant to Fe-deficiency. The *OsDMAS1* promoter contains IDE-2 like elements, suggesting that its expression is regulated by Fe-deficiency. *OsDMAS1* expression was detected in Fe-sufficient roots (**Fig-2.13**), consistent with reports of the detection of DMA in Fe-sufficient rice and barley roots

(Higuchi et al., 2001). *OsNAS1-2* (Inoue et al., 2003) and *OsNAAT1* (Inoue et al., unpublished data) are also expressed in cells that participate in long-distance transport under Fe-sufficient conditions. These results also confirmed that DMA is not only important for Fe acquisition but also essential for Fe homeostasis. In contrast, *HvNAAT-A*, which encodes a protein that converts NA into the 3"-keto intermediate, is not expressed in the presence of Fe, whereas *HvNAAT-B* shows a basal level of expression. The expression of both genes increases under Fe-deficient conditions (Takahashi et al., 1999). *DMAS* expression was upregulated under Fe-deficient conditions in root tissue (**Fig-2.11**), which is important for the production and secretion of DMA. In rice and barley, DMA was detected in shoots under Fe-sufficient conditions and increased under Fe-deficient conditions. More DMA was detected in Fe-deficient and Fe-sufficient rice leaves than in barley (Higuchi et al., 2001), even though barley secretes higher amounts of MAs (Römheld et al., 1990; Singh et al., 1993). Western blot analysis also confirmed that DMAS protein increases in response to Fe-deficiency in rice, wheat and barley roots. No band was detected in maize. It may be due to the low expression of DMAS in maize. Other reasons may be that antibodies do not recognize ZmDMAS, or in maize it may be posttranscriptionally regulated. It also seems that expression of *DMAS1* in graminaceous plants is not regulated posttranscriptionally for rice, wheat and maize. No expression was observed in leaves of all crops examined under Fe-deficient or sufficient conditions. It may be due to low expression levels as revealed by Northern blot analysis.

No *OsDMAS1* promoter-*GUS* activity was detected in Fe-sufficient leaves. It is possible that the DMA detected in Fe-sufficient rice leaves is translocated from roots in a complex with Fe (Mori et al., 1991). This hypothesis is strengthened by the fact that under Fe-sufficient conditions, *OsDMAS1* expression was only observed in the portions of roots that are involved in long-distance transport. Under Fe-deficient conditions, the amount of DMA increases in rice shoots, and the expression of *DMAS* suggest that DMA is at least partially synthesized in shoot tissue. This DMA is thought to be involved in Fe homeostasis and does not participate in the acquisition of Fe from the soil.

The development of transgenic rice plants that are tolerant of alkaline soils with low Fe availability is important to increase rice production in problem soils. Alkaline soils cover approximately 30% of world's arable land (Chen and Barak, 1982) and rice grown on such soils is prone to Fe-deficiency. Previously a genomic fragment containing two *NAAT* genes from barley were introduced in rice and the resulting transformants produced 4 times more grains as compared with control. The production of DMA was only 1.8 times higher than control, in spite of the 50 fold increase in NAAT activity (Takahashi et al., 2003). This data along with Northern and western blot analysis suggests that in rice low expression of DMAS is limiting factor responsible for the poor growth of rice in alkaline soils. The introduction of *HvDMAS1*, alone or in combination with *NAS*, *NAAT*, *IDS2* and *IDS3*, into rice would be a good strategy to develop transgenic rice plants tolerant to Fe-deficiency

in calcareous soils. On the other hand the plants lacking or over expressing DMAS will reveal the role of DMA in Fe homeostasis.

CHAPTER

3

Cloning and Characterization of Glutathione Reductase from Barley

3.1). Introduction

The tripeptide glutathione (γ-Glu-Cys-Gly; GSH) is a ubiquitous non-protein thiol compound in eukaryotic cells and participates in the regulation of cellular redox status (reviewed by Foyer et al., 2001). GSH is essential for plant growth and is particularly important in plants during exposure to oxidative stress, when reactive oxygen species (ROS) are formed and GSH operates as a central component of the ascorbic acid–GSH cycle (Noctor and Foyer, 1998). Other functions of GSH include the storage and long-distance transport of reduced sulfur (Brunold and Rennenberg, 1997), conjugation with secondary plant metabolites and xenobiotics via glutathione S-transferase (Marrs, 1996; Alfenito et al., 1998), and the formation of phytochelatins in response to heavy metal exposure (Cobbett, 2000). GSH also participates in the control of flowering (Ogawa et al., 2001) and hair tip growth (Sanchez-Fernandez et al., 1997). It is required for the G1 to S phase transition of the cell cycle in roots, and the phenotype of the *rml1* (*rootmeristemless*) mutant, lacking the first enzyme of GSH biosynthesis, is relieved after supplying GSH (Vernoux et al., 2000). Finally, the oxidation status of GSH may also be involved in the signal transduction for the regulation of gene expression and the cell cycle (Noctor et al., 2002); as well as for the aggregation of storage proteins in the endoplasmic reticulum of cereal seeds (Jung et al., 1997).

GSH must be in its reduced form to fulfill many of its roles. This is particularly true when it acts as an antioxidant against ROS such as hydrogen peroxide and super oxide (Noctor and Foyer, 1998). Thus, the enzyme glutathione reductase

(GR) is essential for the functioning of GSH and is a prevalent member of the flavoprotein oxidoreductase family in both eukaryotes and prokaryotes. GR catalyzes the reaction that converts oxidized glutathione (GSSG) to reduced glutathione (GSH) using NAD(P)H as an electron donor (Meister, 1988), (**Fig-3.1**). In plants, GR plays a key role in the response to oxidative stress by maintaining the intracellular pool of GSH. Expression of GR is upregulated under stresses, such as changes in salinity, drought, high light intensity, mechanical wounding, chilling, and exposure to heavy metals and herbicides (Foyer et al., 1991; Mullineaux and Creissen, 1997; Apel and Hirt, 2004; Romero-Puertas et al., 2006).

Fe is an essential element in plants, and is required for cellular events such as respiration, chlorophyll biosynthesis, and photosynthetic electron transport. Fe is required for the synthesis of heme and chlorophyll. Indeed, low chlorophyll content (chlorosis) of young leaves is the most obvious visible symptom of Fe-deficiency. A number of heme and non-heme proteins involved in redox systems also require Fe. The most well-known heme proteins are cytochromes, which contain Fe as a prosthetic group. Other heme enzymes such as catalase and peroxidase also depend on Fe for their activity. In non-heme proteins such as those containing Fe–S domain, Fe associates with the thiol group of cysteine, with inorganic sulfur in clusters, or with both, such as in ferredoxin. Isozymes of superoxide dismutases (SOD), which detoxify superoxide anions, also require Fe as a prosthetic group. The activities of catalase, peroxidase (Iturbe-Ormaetxe et al., 1995; Tewari et al., 2005), and ascorbate peroxidase (Iturbe-Ormaetxe et al., 1995; Ishikawa et al.,

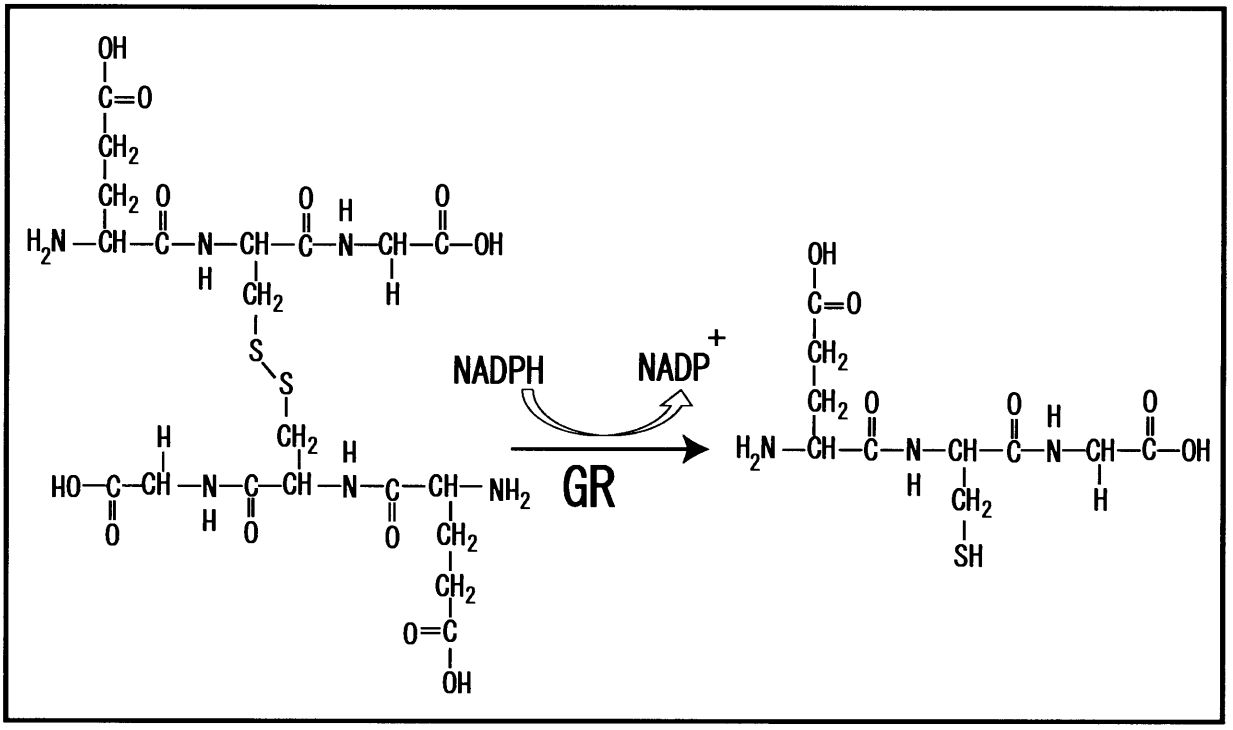

Fig-3.1: Reduction of Glutathione Disulphide (GSSG) to Glutathione (GSH) by Glutathione Reductase (GR)

2003; Zaharieva et al., 2004; Tewari *et al.,* 2005) decrease under Fe-deficient conditions, whereas the activities of different isozymes of SOD increase (Tewari *et al.,* 2005). These enzymes play a role in scavenging ROS; thus Fe-deficiency, like Zn-deficiency (Cakmak and Marschner, 1988), can trigger secondary oxidative stress.

Although Fe is abundant in soil, it is mainly present in oxidized Fe(III) compounds, which are poorly soluble in neutral to alkaline soils as discussed in **section-1**. As such, Fe-deficiency is a worldwide problem that is responsible for serious reductions in crop yields. The molecular basis of Fe-acquisition from soil has been identified and strategies have been proposed to overcome this problem (review in Takahashi, 2003). Although excess Fe is known to trigger oxidative stress (Halliwell and Gutteridge, 1986), little is known about the role of Fe-deficiency-induced oxidative stress and the role of antioxidants such as GSH in plant responses to Fe-deficiency. Therefore, understanding the mechanisms involved in the Fe-deficiency response is of extreme importance to create Fe-deficiency-tolerant plants and to thereby increase crop production.

The expression of GR is regulated by a variety of biotic and abiotic stresses; however, to date no report has described the expression pattern of GR in response to Fe-deficiency stress in plants. These responses are especially of interest in barley, which is the most Fe-deficiency-tolerant species among graminaceous crops. To investigate the regulation of GR in graminaceous plants, cytosolic and chloroplastic isoforms were cloned from barley and their expression patterns, as

well as enzyme activities were examined under Fe-sufficient and Fe-deficient conditions in graminaceous plants.

3.2). Experimental procedures

3.2.1). Cloning of *HvGR1* and *HVGR2*

A cDNA library prepared from Fe-deficient barley roots (Higuchi et al., 2001) was screened to clone the full-length cDNA of barley cytosolic GR (*HvGR2*). Two cDNA clones containing partial sequences of cytosolic GR (AB063248 and AB063249) were isolated using degenerate primers **(Fig-2.1)**. The ORF of AB063248 was labeled with ^{32}P, and approximately 200,000 colonies of the cDNA library were screened through colony hybridization as described previously (Higuchi et al., 2001).

Partial sequences of barley chloroplastic GR (*HvGR1*) were identified as unigene numbers 7437 and 37686 in the HarvEST database (Version 1.47; http://harvest.ucr.edu/) because of their strong homology to rice chloroplastic GR (*OsGR1*; LOC_Os03g06740). The *HvGR1* ORF was amplified from the cDNA library using the 5'-caccATGGCGACAACCGCGGCCCTCCC-3' and 5'-TACTTCTGAGCGACGACCTCATC-3' as forward and reverse primers respectively. The amplified cDNA clone was subcloned into pENTR/D-TOPO (Invitrogen, Carlsbad, CA) and sequenced using a Thermo Sequenase Cycle Sequencing Kit (Shimadzu, Kyoto, Japan) and a DSQ-2000L DNA sequencer (Shimadzu). The nucleotide sequences of *HvGR1* and *HvGR2* were submitted to the DDBJ/GenBank/EBI Data Bank with accession numbers AB277096 and AB277097. The rice genome database (http://www.tigr.org/) was explored to determine the number and location of GR genes in the rice genome.

3.2.2). Northern blot analysis

Seeds of barley (*Hordeum vulgare* L. cv. Ehimehadaka no. 1), wheat (*Triticum aestivum* L. cv. Chinese spring), maize (*Zea mays* cv. Alice), and rice (*Oryza sativa* L. cv. Nipponbare) were germinated on wet filter paper and cultured as described by Kanazawa et al. (1994). For the Fe-deficiency treatments, plants were transferred to culture solution lacking Fe. Symptoms of Fe-deficiency were apparent after 2 weeks, at which point the roots and leaves were harvested, frozen in liquid nitrogen, and stored at –80°C until use. Samples were also collected every 3 h to examine whether the expression of GR follows a diurnal rhythm under Fe-sufficient and Fe-deficient conditions.

Total RNA was extracted from roots and shoots, and 10 μg were electrophoresed in 1.2% (w/v) agarose gels containing 0.66 M formaldehyde and transferred to Hybond-N+ membranes (Amersham, Piscataway, NJ). For *GR1*, the full length ORF of *HvGR1* was labeled with digoxigenin (DIG) through PCR and used as a probe for Northern blot analysis. For *GR2*, Northern blot analysis was performed with four different probes: the 5'-region of *HvGR2* amplified with the forward and reverse primers as 5'-ATGATCGAAGGAGCAGGAA-3' and 5'-CCAGTTGTAGTTGATGTCCCCGTTGAT-3' respectively, the 3'-region of *HvGR2* amplified with the forward and reverse primers as 5'-TGATGCTGAGACCGATAA-3' and 5'- GCTTGGAAATCACAACAATAC-3' respectively, and the full length ORF of *HvGR2* labeled with DIG. For *OsGR2*, a full length ORF was cloned from a rice cDNA library with the forward and reverse

primers as 5'-ATGGCTAGGAAGATGCTCAAGG-3' and 5'-CTACAAGTTTGTCTTTGGCTTGG-3' respectively, then sequenced using a Thermo Sequenase Cycle Sequencing Kit (Shimadzu) and a DSQ-2000L DNA sequencer (Shimadzu), and labeled with DIG. Each probe was individually incubated with each membrane at 68°C and processed as described previously (Engler-Blum et al., 1993; Yoshihara et al., 2003).

3.2.3). Determination of GR activity

To subclone *HvGR1* into pMAL-c2 (New England Biolabs, Beverly, MA), the ORF was amplified with primers such that it contained an *Xba*I site at the 5' end and a *Hin*dIII site at the 3' end. The ORF was amplified, subcloned into pCR-Blunt II-TOPO (Invitrogen), and sequenced. The resulting plasmid was then digested with *Xba*I and *Hin*dIII and the excised fragment containing *HvGR1* was subcloned into pMAL-c2. This plasmid was designated pMAL-c2-*HvGR1*. *HvGR2* and AB063249 were also subcloned into pMAL-c2 in the same manner. These pMAL-c2 plasmids were introduced into *E. coli* XL1-Blue, which were induced to produce the recombinant fusion proteins. The proteins were purified as described by Higuchi et al. (1999). The GR activity was determined using 1μg of recombinant HvGR1, HvGR2, and AB063249 bound to a maltose-binding protein with a GR assay kit (Trevigen, Gaithersburg, MD) according to the manufacturer's instructions with the exception, that disposable cuvettes were used instead of quartz cuvettes. The GR assay was performed at room temperature and the GR specific activity was calculated based on decrease in absorbance at 340 nm over a period of 5 minutes

using Ultrospec 3300 pro (Amersham Biosciences). The GR specific activity was calculated with formula

$$\text{GR activity (mU)} = \frac{\Delta \text{ A 340 nm/min}}{6.22 \times 10^{-3} \text{ ml/nmol}}$$

where 6.22×10^{-3} is molar extinction coefficient for NADPH at 340 nm. One mU of GR is equal to 1 nm NADPH consumed/min.

To determine the effect of Fe-deficiency on total GR activity in rice, wheat, barley, and maize, the crude protein extract from plants grown under Fe-sufficient and Fe-deficient conditions was extracted using the buffer provided with the kit according to the manufacturer's instructions (Trevigen). The proteins were quantified using the Bradford assay (Bradford, 1976) and diluted to 1 μg μl^{-1} with dilution buffer. Each assay was performed in duplicate with 40 μg of total purified protein.

3.2.4). Subcellular localization of glutathione reductase

HvGR2, AB063248 and AB063249 were amplified with forward and reverse primers without stop codon and the amplified fragments containing the respective coding sequences was subcloned into pENTR/D-TOPO (Invitrogen, Carlsbad, CA). The pENTR/D-TOPO entry vector containing the *HvGR2* coding sequence was designated pENTR- *HvGR2* and so on. The plasmid pDEST35S-sGFP (Ishimaru et al., 2005) was used as destination vector. A subsequent attL substrate and attR substrate recombination reaction (Invitrogen) between the destination and entry vectors generated an expression clone containing the gene encoding

35S-HvGR2-sGFP. Onion epidermal cells were transformed using the Biolistic PDS-1000/He Particle Delivery System (Bio-Rad, Tokyo, Japan), and the sGFP fluorescence was visualized as described by Mizuno et al. (2003). The subcellular localization of HvGR1 and HvGR2 were also predicted with the help of computer software pSORT (http://psort.ims.u-tokyo.ac.jp/).

3.3). Results

3.3.1). Cloning of *HvGR1* and *HvGR2*

The two cDNA clones AB063248 and AB063249 were isolated from a cDNA library prepared from Fe-deficient barley roots and were highly homologous to rice and wheat GR. These clones were isolated in an attempt to isolate the gene for deoxymugineic acid synthase (DMAS) using degenerate primers (**Fig-2.1**); however, no DMAS activity was detected (data not shown). The full-length cDNA library was screened using AB063248 as a probe and isolated two cDNA clones: one corresponding to AB063249 and one for cytosolic GR (*HvGR2*). The *HvGR2* contained the full length of AB063248 and AB063249 **(Fig-3.2)** with some variation at the 5' UTR region. This type of variation was also observed for *HvGR2* where more than one clones were identified with identical ORF while varying length of nucleotides at 5' UTR (Data not shown). The chloroplast GR (*HvGR1*) was cloned with primers designed to amplify the *HvGR1* ORF. The sequence of GR was highly conserved among graminaceous plants and *HvGR1* showed 86% homology to rice chloroplastic GR. Likewise, *HvGR2* showed high homology to wheat (*Triticum monococum*; 96%) and rice (89%) cytosolic GR (**Fig-3.3**). Three genes for GR exist in rice (**Fig-3.3**). The gene for cytosolic GR (*OsGR2*) is located on rice chromosome 2 and is split into 16 exons (**Fig-3.3b**), whereas rice chloroplastic GR (*OsGR1*) is located on chromosome 3 and split into 10 exons (**Fig-3.3c**). Rice was also found to contain a partial sequence for *GR1* located on chromosome 10 (**Fig-3.3d**). This sequence lacked a FAD-binding domain and part of the NADPH-binding domain.

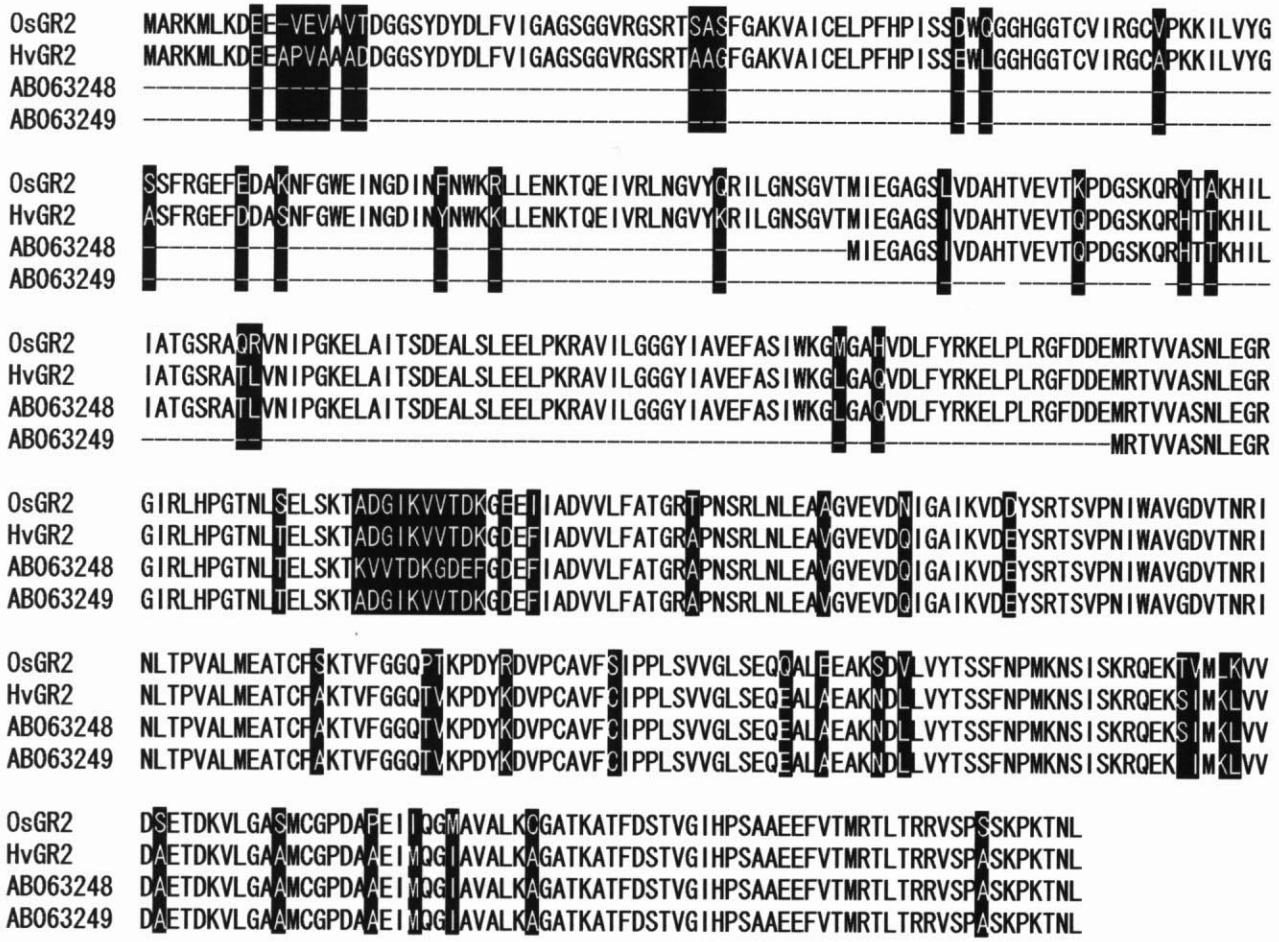

Fig-3.2: Amino Acid Sequence of Cytosolic GR

The letter with black background shows the variation in sequence.

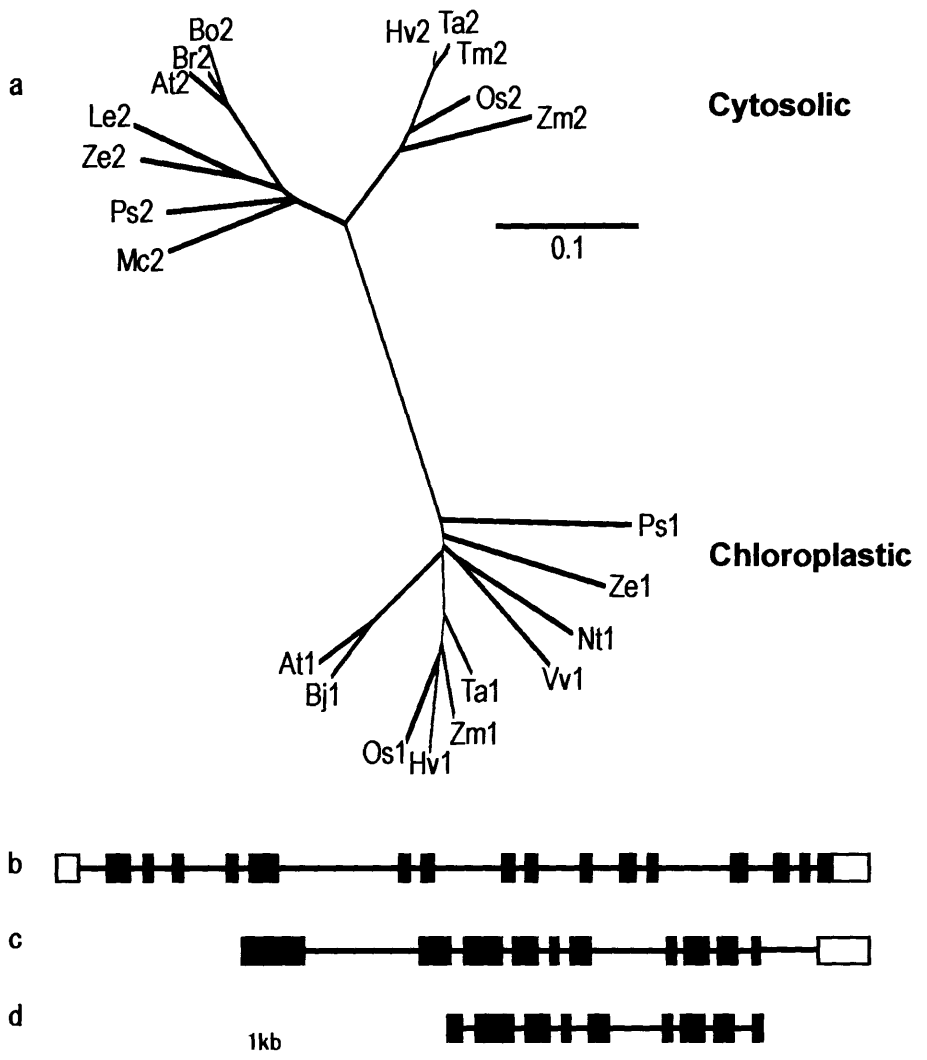

Fig-3.3: Phylogency and genomic structure of GR in rice

a; Unrooted phylogenic tree of GR

Hv, Hordeum vulgare; Ta, Triticum aestivum; Tm, T. monococum; Os, Oryza sative; Zm, Zea mays; Bo, Brassica oleracea; Br, Brassica rapa; At, Arabidopsis thaliana; Le, Lycopersicum esculentum; Ze, Zinnia elegans; Ps, Pisum sativum; Mc, Mesembryanthemum crystallinum; Nt, Nicotiana tabacum; Vv, Vitis vinifera; Bj, Brassica juncea. Numbers 1 and 2 represent chloroplastic and cytosolic GR respectively.

b: Genomic structure of rice cytosolic GR

c: Genomic structure of rice chloroplastic GR

d: Genomic structure of rice partial chloroplastic GR

White boxes show exons and black boxes represent untranslated regions.

This sequence is however slightly larger than AB063248 and AB063248 and have more homology to OsGR1 as compared to OsGR2.

Based on their nucleotide sequences, *HvGR1* and *HvGR2* were predicted to encode polypeptides of 550 and 497 amino acids, respectively (**Fig-3.4**). The NADPH and substrate-binding domains were identified by aligning the sequences with those of other GRs that had been characterized previously. Similar to other GRs, these domains were conserved for graminaceous *GR1* and *GR2*.

3.3.2). Enzyme activity

HvGR1 and *HvGR2* were expressed in *E. coli* as a maltose-binding fusion protein, size was confirmed with SDS PAGE (**Fig-3.5a**) and purified proteins were tested for the ability to reduce GSSG. AB063249 was also expressed as a maltose-binding protein; however, it lacked a complete FAD-binding domain and part of the substrate-binding domain, and was therefore used as a negative control. HvGR1 and HvGR2 were shown to catalyze the conversion of GSSG to GSH (**Fig-3.5b**) as measured by the decrease in absorbance of NADPH at 340 nm. The enzyme activity for HvGR1 was three times higher than that of HvGR2. No enzyme activity was observed for AB063249.

3.3.3). The expression of GR1 and GR2 under Fe-deficient conditions

Northern blot analyses were performed to determine whether AB063248 and AB063249 are expressed under Fe-deficient conditions. Results showed that these clones are expressed as only a single band of approximately 2kb corresponding to

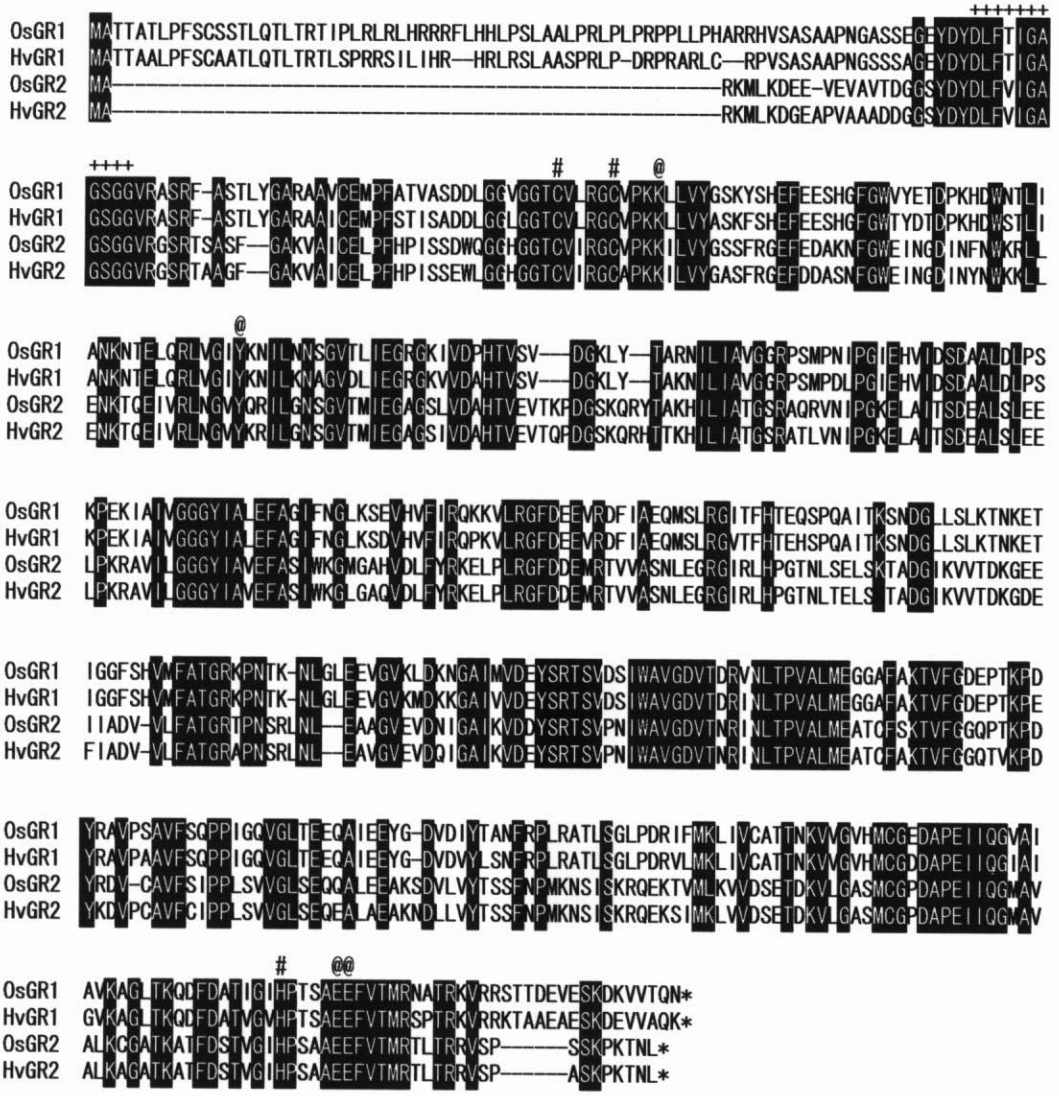

Fig. 3.4: Sequence Homology between Rice and Barley GR

#: GSSG-binding domain; +: NAD(P)H-binding domain;
@: FAD-binding domain. * represents stop codon.

The letters with black background highlight the conserved regions

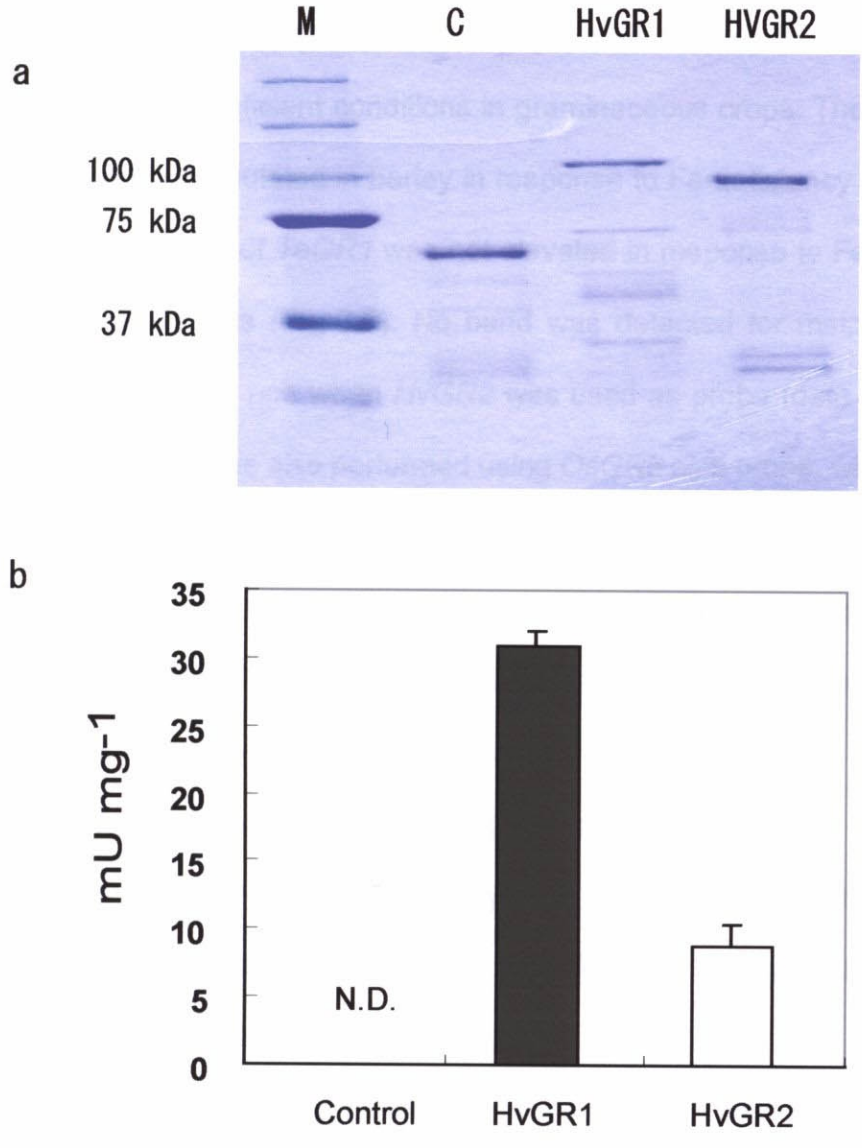

Fig-3.5: GR Activity of HvGR1 and HvGR2

a: SDS page of purified recombinant GR proteins. M: size marker, C: AB063249.

b: Glutathione reductase activity of recombinant HvGR1 and HvGR2 Recombinant AB063249 protein lacking FAD binding domain and part of NADPH binding domain was used as negative control. N.D.: Not detected.

HvGR2 was observed in all cases (Data not shown). Further more Northern blot analysis were performed to check whether the expression of *GR1* and *GR2* was upregulated under Fe-deficient conditions in graminaceous crops. The expression of both genes was upregulated in barley in response to Fe-deficiency (**Fig-3.6**). In addition, the expression of *TaGR1* was not elevated in response to Fe-deficiency, while that of *TaGR2* was (**Fig-3.6**). No band was detected for maize, and faint bands were detected for rice when *HvGR2* was used as probe (data not shown). Northern blot analysis was also performed using *OsGR2* as a probe, which showed that the expression of OsGR2 decreased slightly under Fe-deficient conditions (**Fig-3.6b**), however; in case of maize, no band was detected with all probes used. The expression of *HvGR1* was mainly localized to shoot tissues and only slight expression was observed in roots. Conversely, the expression of *HvGR2* was mainly observed in roots, where it was significantly upregulated in response to Fe-deficiency. Although Northern blot analysis using *OsGR1* as a probe was not attempted, microarray analysis showed that *OsGR1* is upregulated under Fe-deficient conditions (data not shown).

Northern blot analysis using the *HvGR1* probe detected two bands (~2 kb and ~1.5 kb; **Fig-3.6a**). The smaller fragment may have been the partial sequence of *HvGR1*. Only one band representing a ~2-kb fragment was detected using *HvGR2* as a probe.

Northern blot analysis was also performed for the samples collected every 3 h after sunrise. The results showed that the expression of *HvGR2* was regulated in a

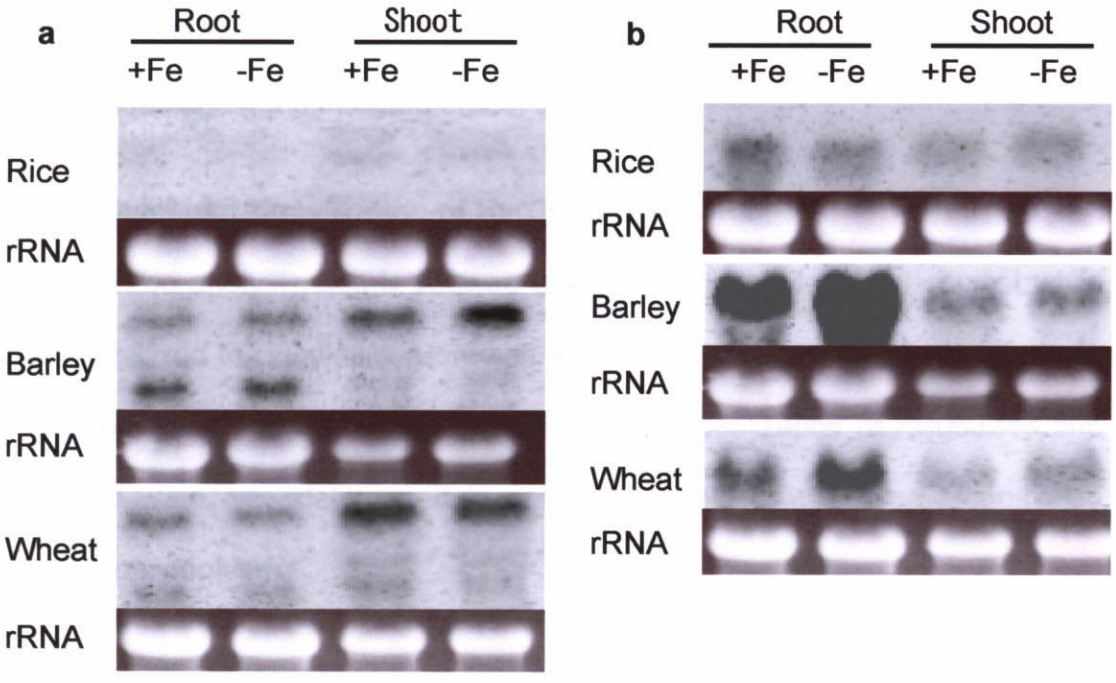

Fig-3.6: Northern Blot Analysis for GR1 and GR2 in Graminaceous Plants

a) Northern blot analysis for chloroplastic GR (GR1). *HvGR1* was used as a probe.
b) Northern blot analysis for cytosolic GR (GR2). *HvGR2* was used as a probe for barley and wheat. *OsGR2* was used as a probe for rice.

diurnal fashion under both Fe-deficient and Fe-sufficient conditions (**Fig-3.7**). Under Fe-deficient conditions, *HvGR2* expression slightly decreased immediately following sunrise then increased approximately 6 h later. Under Fe-sufficient conditions, *HvGR2* expression increased with the sunrise, declined 6 h into daylight, and increased again 9 h after the end of illumination.

3.3.4). Subcellular Localization of HvGR1 and HVGR2

In silico analysis clearly showed that HvGR1 localizes to chloroplast while HvGR2 localized to cytoplasm. Moreover the HvGR2-sGFP localized to cytoplasm in onion epidermal cells (**Fig-3.8**). The subcellular localization of AB063248 and AB063249 were also determined in onion epidermal cells. These clones also localized to cytoplasm.

3.3.5). GR activity increases in response to Fe-deficiency

Total protein was extracted from Fe-sufficient and Fe-deficient barley, wheat, rice, and maize. GR activity increased in barley (×1.9), wheat (×1.2), and in maize (×3.0) root tissues with Fe-deficiency (**Table-4**). The barley and wheat results are in line with those of the Northern blot analysis, whereas GR activity slightly decreased in rice roots (×0.87). GR activity increased in rice (×1.5), barley (×1.3), and maize (×3.0) shoot tissues. These results correspond with the Northern blot analyses for wheat, barley, and rice. No band was detected in maize, likely because we lacked a maize-specific probe. However, the GR activity increased in response to Fe-deficiency in maize roots and shoots. As results showed (**Fig-3.6 and Table-4**)

that in roots GR2 and in shoots GR1 is mainly responsible for the enzyme activity, it raised the possibility that expression of GR1 and GR2 increase in maize in response to Fe-deficiency. The enzyme activity was higher in root tissue than shoot tissue for all species examined.

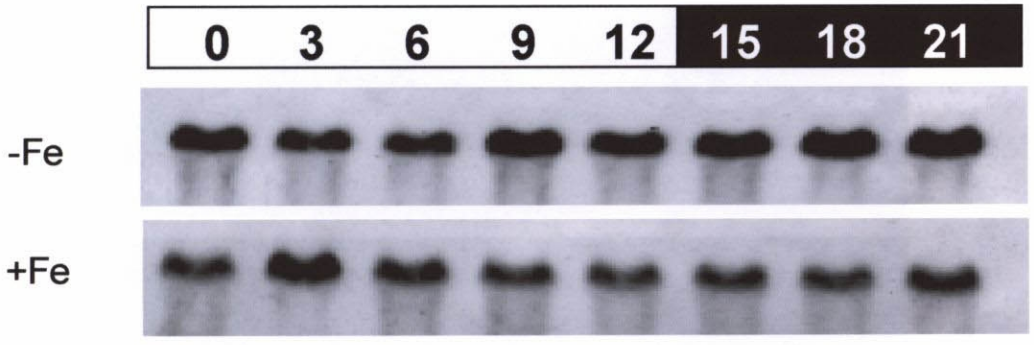

Fig-3.7: Northern Blot Analysis Showing Diurnal Changes in Expression of HvGR2

Numbers above the figure show the number of hours after illumination. The white box represents the lights on time while the dark box represents time after the lights had been turned off.

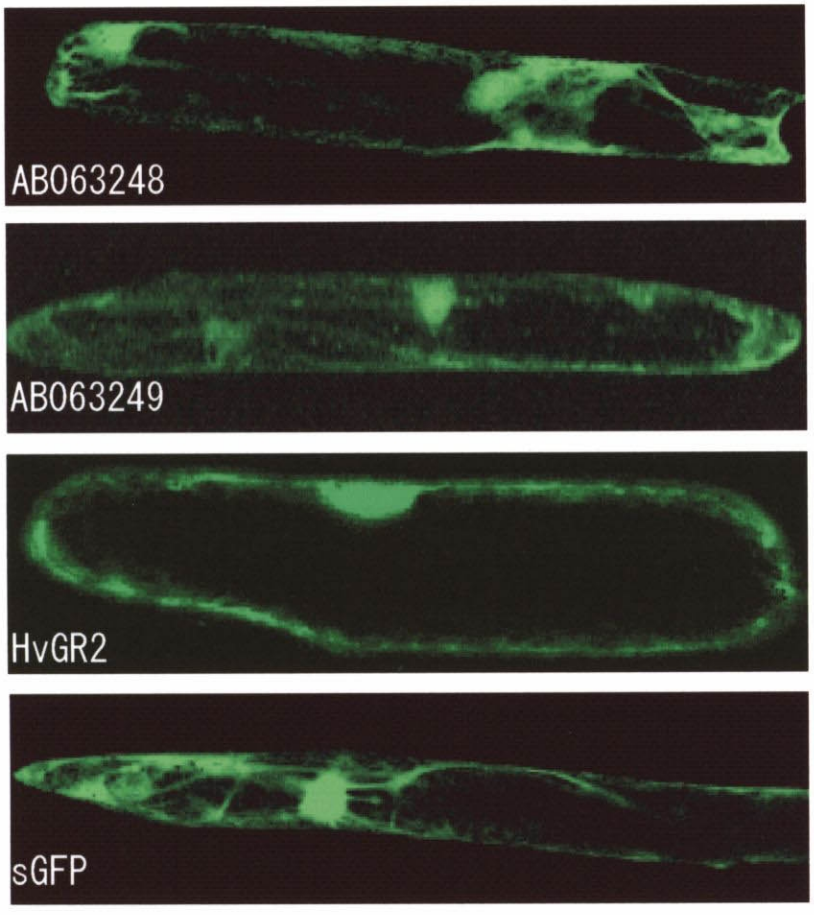

Fig-3.8: Subcellular Localization of HvGR2 in Onion Epidermal Cells

AB063248, AB063249 and HvGR2 were transiently expressed in onion epidermal cells. Transiently expressed sGFP was used as a control.

Table-4: GR Activity in Response to Fe-deficiency Stress (mU/mg crude extract)

	ROOT			SHOOT		
	+Fe	-Fe	Ratio	+Fe	-Fe	Ratio
Rice	125 ± 14.1	109 ± 5.2	0.9	52 ± 0.3	79 ± 0.3	1.5
Barley	150 ± 17.6	278 ± 5.1	1.9	51 ± 0.3	65 ± 0.6	1.3
Wheat	117 ± 11.4	145 ± 6.8	1.2	75 ± 0.6	76 ± 0.3	1.0
Maize	36 ± 4.5	110 ± 0.3	3.0	21 ± 0.3	62 ± 1.4	3.0

3.4). Discussion

In present study the genes for chloroplastic (*HvGR1*) and cytosolic (*HvGR2*) GR in barley were cloned. GR is a ubiquitous enzyme that has been cloned from a number of prokaryotic and eukaryotic species (e.g., Greer and Perham, 1986; Edwards et al., 1990; Foyer et al., 1991, Creissen et al., 1992). The sequences of cytosolic and chloroplastic GR are conserved among graminaceous crops (**Fig-3.4**). The *HvGR2* and *TaGR2* genes were mainly expressed in root tissue and a light band was observed in shoot tissue. Similar expression patterns were observed for *OsGR1* in that expression was mainly observed in root and calli, rather than in leaves (Kaminaka et al., 1998). Conversely, the expression of *PsGR2* was very low in root tissue and high in shoots and flowers (Stevens et al., 1997; Romero-Puertas et al., 2006). These results suggest that the expression of graminaceous and non-graminaceous GR may be regulated differently. It has also been reported that the expression of *PsGR1* and *PsGR2* are regulated differentially in response to various stresses such as mechanical wounding and increased temperature (Romero-Puertas et al., 2006). In barley, both *HvGR1* and *HvGR2* were upregulated by Fe-deficiency, whereas wheat exposed to the same conditions only exhibited increased levels of *TaGR2*.

Although expression of *GR* in response to abiotic stresses was not investigated in present studies, studies using the differential display protocol showed that the expression of *HvGR2* is upregulated under salt stress (Ueda et al., 2002). GR specific activity was also measured to determine whether this enzyme is regulated

posttranscriptionally. The *ZmGR1* is posttranscriptionally regulated in bundle sheath cells (Pastori et al., 2000), as are *PsGR1* and *PsGR2* in response to various abiotic stresses (Romero-Puertas et al., 2006). Increased GR activity in Fe-deficient barley, wheat, and maize roots and Fe-deficient rice, barley, and maize leaves was observed. The expression of *HvGR1* was mainly localized to shoot tissues and that of *HvGR2* to root tissues. Northern blot analyses for barley and wheat revealed that the upregulation of gene expression is directly proportional to the increase in GR-specific activity. Therefore, it may be concluded that the increased GR activity in shoot tissue was due to the upregulation of *HvGR1*, whereas the increase in root tissue may have been a result of the upregulation of *HvGR2*. Moreover, the expression and enzyme activity for *OsGR2* decreased in response to Fe-deficiency. These results suggest that *GR1* and *GR2* genes are not posttranscriptionally regulated in rice, wheat, or barely. No band was detected for maize using Northern blot analysis, likely because *HvGR1* and *HvGR2/OsGR2* were used as probes. The GR specific activity, however, clearly showed that the gene is upregulated in Fe-deficient maize root and shoot tissues.

GR may allow plants to cope with Fe-deficiency in a variety of ways. Redox systems using heme and non-heme proteins such as cytochromes, catalase, peroxidases, and ferredoxin require Fe. Thus, under Fe-deficiency stress, the activity of these enzymes declines. GSH scavenges ROS via the Asc–GSH cycle and glutathione peroxidase (GPX). Although the Asc–GSH cycle is down-regulated under Fe-deficient conditions (Zaharieva and Abadía 2003), given that the activity

of SOD increases (Tewari *et al.*, 2005), GR may play a role in coping with Fe-deficiency-induced oxidative stress through the GPX cycle in combination with SOD (**Fig-3.9**). It should be noted that the oxidative stress induced by Fe-deficiency is fundamentally different from that induced by salt or heavy metal stress, whereby the production of ROS as well as the activities of catalase and peroxidases increase (Patra and Panda, 1998; Kim et al., 2005). When present in excess, Fe produces ROS thorough Fenton reaction

$$H_2O_2 + Fe^{2+} \longrightarrow Fe^{3+} + OH^- + OH^{\cdot}$$

leading to oxidative stress. However it seems that under Fe-deficient conditions, the production of ROS does not increase significantly, rather oxidative stress occurs as the activities of some enzymes involved in scavenging ROS decrease.

GR may also play a role in internal Fe homeostasis. Mobilization of Fe may help plants cope with Fe-deficiency stress. Graziano et al. (2002), and Graziano and Lamattina (2005), recently discussed the role of NO in Fe mobilization in plants. Interestingly, the ability of NO to induce Fe mobilization is dependent on GSH while that of chelators is independent of GSH (Watts and Richardson, 2001). This suggests that NO alone does not have the capacity to remove Fe from intermediates and that it may require the reducing capacity of GSH. Alternatively, or in combination with this latter mechanism, GSH may form a mixed Fe complex with NO (GS-Fe-NO) in order to acquire the appropriate lipophilicity and charge to diffuse or be transported from the cell (Watts and Richardson, 2002). The presence of dithiol dinitrosyl–Fe complexes within cells has been previously demonstrated

(Vanin, 1991). As part of this complex, GSH may play an important role in signal transduction for the regulation of gene expression in response to different stresses and Fe-homeostasis. Moreover, S-nitrosylated form of GSH has been suggested to act as a transport molecule for NO, thereby increasing its half-life and allowing for effective biological activity (Lipton et al., 2001; Lipton, 2001). GSH is also essential for the acitivity of glutahione S-transferase, which specifically interacts with the dintrosyl-diglutathioneyl–Fe complex and behaves like a storage protein for this complex *in vivo* and *in vitro* (Maria et al., 2003; Turella et al., 2003). These results suggest that GR may play a role in internal Fe homeostasis in graminaceous plants and thereby allow plants to cope with Fe-deficiency.

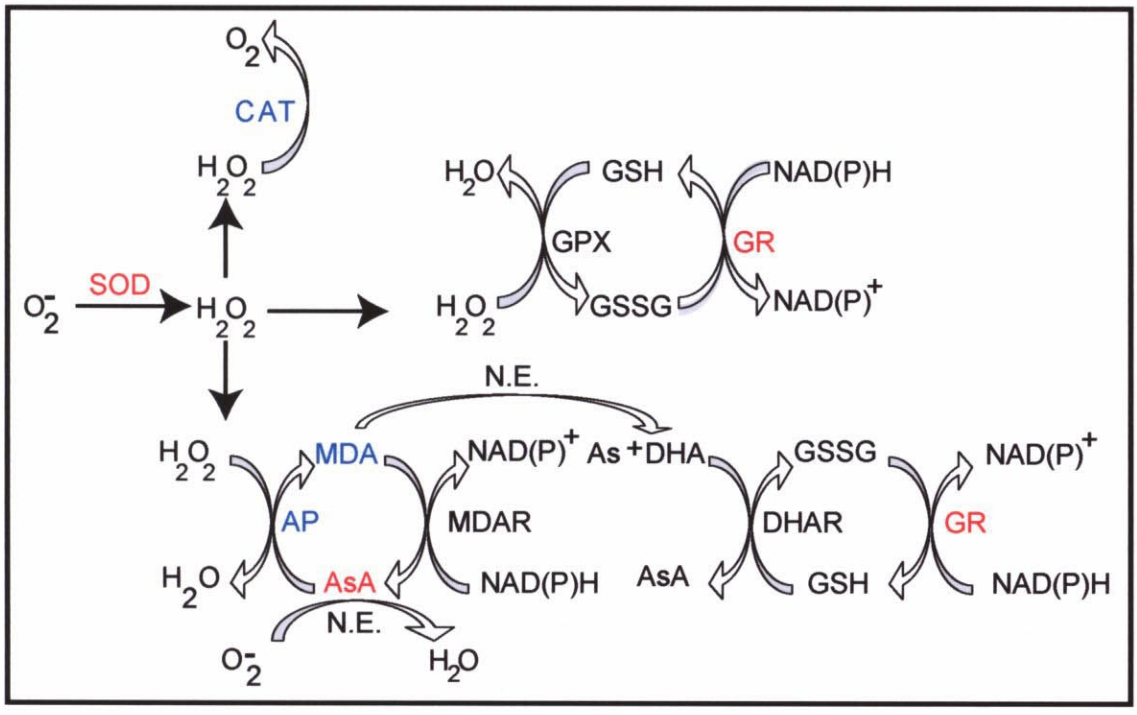

Fig-3.9: The Role of Glutathione in Coping with Fe-deficiency Induced Oxidative Stress

CAT, catalase; GPX, glutathione peroxidase; APX, ascorbate peroxidase; MDA, monodehydroascorbate; AsA, ascorbic acid; MDAR, MDA reductase; DHA, dehydroascrobate; DHAR, DHA reductase; N.E., nonenzymatic reaction.

The activity/amount of the enzymes/compounds shown in red increases under Fe-deficiency, while that of shown in blue decreases.